

superconducting state with a large magnetic field and measured the temperature and magnetic field dependence of the electrical resistivity in fields to 32 T and at temperatures to about 45 mK at the NHMFL/Tallahassee.

Our single crystal sample exhibited a superconducting critical temperature of 0.85 K in zero field and an upper critical field of 9.0 T as  $T \rightarrow 0$ . These resistive transitions were very sharp: about 7 mK wide in zero field and about 0.4 T wide as  $T \rightarrow 0$ , consistent with a very high quality crystal. The field was aligned along the [100] axis.

The transverse magnetoresistance reaches  $-80\%$  at 1.2 K and 33 T. An inflection point is observed at about 4 T in the 1.2 K data, an inflection point which may be related to a proposed field induced magnetic phase transition in  $\text{UBe}_{13}$ .<sup>2</sup>

Measurements of the temperature dependence of the resistivity over a temperature range of about 50 mK to 1.1 K were made in several fixed fields from 12 to 32 T. In all fields the resistivity shows the low temperature  $T^2$  behavior characteristic of a Fermi liquid. The temperature at which the resistivity deviates from

this quadratic behavior decreases somewhat with increasing field, a behavior which suggests that the zero field ground state of this material is that of a Fermi liquid (unless there is a very strong field dependence to the high temperature limit of the  $T^2$  behavior below 12 T).

It has been noted that the coefficient of the  $T^2$  term in the resistivity ( $A$ ) is proportional to the square of the coefficient of the  $T$ -linear term in the specific heat ( $\gamma$ ) in many systems.<sup>3</sup> Thus we expect the effective mass of this material to vary like  $A^{1/2}$ . Above 25 T we find that  $A^{1/2}$  falls off like  $1/B$ , and extrapolates to zero near 54 T. Our results therefore suggest the destruction of the heavy fermion state in  $\text{UBe}_{13}$  at 54 T. One might expect to see a change in sign of the differential magnetoresistance near 54 T if this suggestion is correct. Measurements in pulse fields are planned to test this prediction.

<sup>1</sup> Stewart, G.R., *Rev. Mod. Phys.*, **56**, 755 (1984) and references therein.

<sup>2</sup> Schmiedeshoff, G.M., *et al.*, *Phys. Rev. B*, **48**, 16417 (1993).

<sup>3</sup> Aronson, M.C., *et al.*, *Phys. Rev. Lett.*, **63**, 2311 (1989); and references therein.

## MOLECULAR CONDUCTORS

### Sensitivity of Fermi Surface Traversal Resonance to the Density-Wave Transition in $\alpha\text{-(BEDT-TTF)}_2\text{KHg(SCN)}_4$

Ardavan, A., Univ. of Oxford, Physics

Schrama, J.M., Univ. of Oxford, Physics

Singleton, J., Univ. of Oxford, Physics

Kurmoo, M., Institut de Physique et Chimie des Matériaux de Strasbourg, (IPCMS), France

Day, P., The Royal Institution, London

Among the great variety of groundstates exhibited by metals based on the molecule BEDT-TTF, the groundstate found in  $\alpha\text{-(BEDT-TTF)}_2\text{KHg(SCN)}_4$ <sup>1</sup> has generated particular interest. This material was generally accepted to form a spin-density-wave at temperatures below about 8 K and magnetic fields below 23 T, but recent work has cast doubt over this;<sup>2</sup> the nature of the density-wave is not clear. It is known, however, that in the low temperature, low magnetic field state, the periodicity of the density-wave causes a reconstruction of the Fermi surface into highly warped quasi-one-dimensional (Q1D) sheets and small quasi-two-dimensional (Q2D) pockets.

We have studied the low temperature, low field state using Fermi-surface traversal resonance (FTR) to characterize the details of the warping of the Q1D sheet.<sup>3</sup> Owing to the Lorentz force, the effect of a magnetic field applied parallel to the plane of the Q1D Fermi sheet is to cause carriers to sweep across

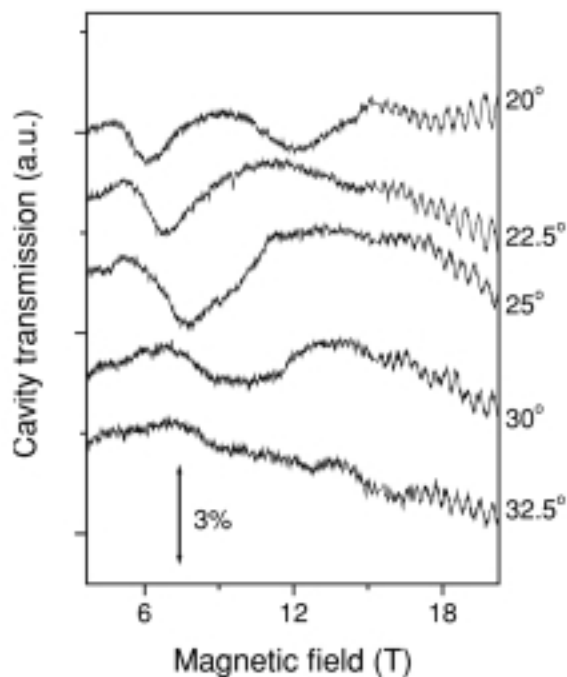


**Figure 1.** FTR in  $\alpha\text{-(BEDT-TTF)}_2\text{KHg(SCN)}_4$ ; amplitude cavity transmission at 70 GHz and 0.6 K as a function of magnetic field for a range of magnetic field angles from 20 to 32.5 degrees.

the sheet. As they do so, the warping of the sheet causes the real-space velocity of the carriers to oscillate with a frequency that is characteristic of the path taken across the sheet. The oscillatory real-space velocity generates resonances in the high frequency conductivity of the material,  $\sigma(\omega)$ , when  $\omega$  matches

the velocity-oscillation frequency. Each warping component in the Fermi sheet generates a resonance; a measurement of the angle-dependence of FTR constitutes a measurement of the Fourier transform of the Fermi sheet.<sup>3</sup>

Given its origin in the Q1D Fermi surface sections, FTR is expected to be sensitive to the Fermi surface reconstruction that occurs at the density-wave transition. At NHMFL, we were able to follow FTR in  $\alpha$ -(BEDT-TTF)<sub>2</sub>KHg(SCN)<sub>4</sub> to high fields using our rotating-resonant cavity system. Figure 1 shows the amplitude cavity transmission at 70 GHz and 0.6 K as a function of magnetic field for a range of magnetic field angles from 20 to 32.5 degrees; in this angle range the positions of FTRs, which appear as minima in the cavity transmission, are very strongly angle-dependent.<sup>3</sup> At fields above 15 T, Shubnikov-de Haas oscillations are visible. The minima visible at lower fields are attributed to FTR, in agreement with earlier studies.<sup>3</sup> With increasing angle, the FTRs move to higher field. The data presented here demonstrate that the FTR amplitude decreases rapidly as the resonant field increases above 15 T; this is a somewhat lower field than the density-wave transition field of about 23 T.<sup>1</sup> A probable explanation is that the density-wave becomes unstable at fields of around 15 T. Fluctuations in the density-wave then reduce the coherence time of carriers traversing the reconstructed Fermi surface. Since it is a resonant effect, FTR is very sensitive to this time; the precursor fluctuations act to destroy FTR well before the density-wave phase transition.

<sup>1</sup> For a recent review see Harrison, N. *et al.*, J. Phys.: Condens. Matter, **11**, 7227 (1999).

<sup>2</sup> Harrison, N., Phys. Rev. Lett., **83**, 1395 (1999).

<sup>3</sup> Ardavan, A., *et al.*, Phys. Rev. Lett., **81**, 713 (1998).

## Angular Dependent Magnetoresistance in (DMET-TSeF)<sub>2</sub>X System

Biskup, N., NHMFL

Brooks, J.S., NHMFL/FSU, Physics

Kato, R., RIKEN, Japan

Oshima, K., Okayama, Japan

The (DMET-TSeF)<sub>2</sub>X family (where X stands for AuI<sub>2</sub>, AuCl<sub>2</sub>, AuBr<sub>2</sub>,...) is a novel charge transfer system that we examined to gain a new insight in field induced spin density wave phenomena (FISDW). We studied two members of the family: X = AuCl<sub>2</sub> and X = AuI<sub>2</sub>. Here we report angular dependent magnetoresistance (AMR) at T = 25 mK and in fields up to 18 T. AMR in AuCl<sub>2</sub> is affected predominantly by commensurability effects that are manifested in a series of pronounced Lebed dips. The angles in an orthorhombic approximation are given by:

$$\tan(\theta) = pc/qb.$$

The FISDW for both compounds is induced at lowest fields when the field is parallel to the b-axis ( $\theta = 0^\circ$ ). The amplitude

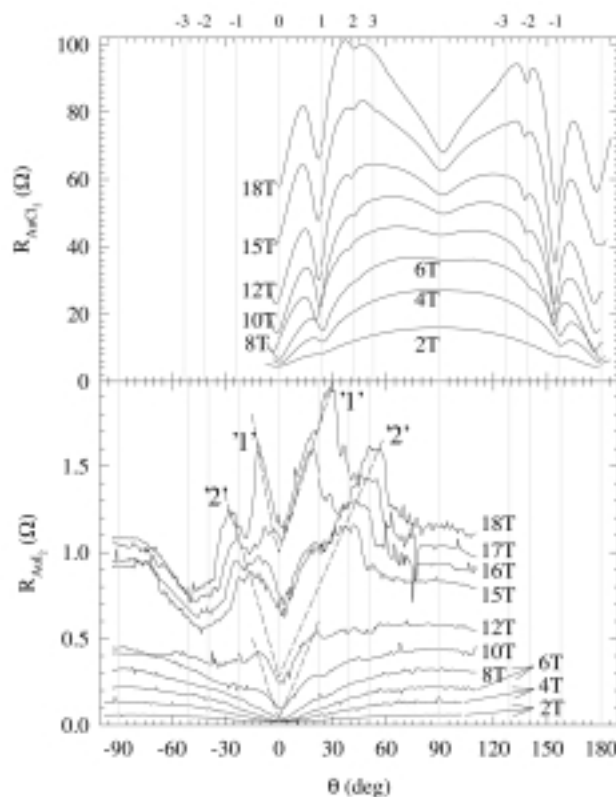


**Figure 1.** AMR for AuCl<sub>2</sub> (upper) and AuI<sub>2</sub> (lower) panel. Vertical lines indicate Lebed angles for indexes p/q given above. In the lower panel, numbers in quotes indicate number n of corresponding FISDW maximum. Dashed lines are guides to the eye for shift of these maxima.

of FISDW transitions (and consequently the magnetoresistance itself) increases with tilt angle<sup>1</sup>, but due to usual orbital (1/cos( $\theta$ )) dependence, FISDW transitions diminish close to  $\theta = 90^\circ$ . At higher fields in AuCl<sub>2</sub>, this is manifested in a wide dip around  $\theta = 90^\circ$ .

In the case of AuI<sub>2</sub>, only slight traces of p/q = 0,1 are observed. Complex angular structure appears in the b-c plane as a consequence of FISDW. Dashed lines are guides to the eyes for shift of these maxima, starting at  $\theta = 0^\circ$  where lowest FISDW transitions are observed. This implies continuous shift of the nesting vector in the b-c plane<sup>2</sup> in a given FISDW quantum state.

<sup>1</sup> Biskup, N., *et al.*, Phys. Rev. B, **60**, 15005 (1999).

<sup>2</sup> Biskup, N., *et al.*, submitted to Phys.Rev.Lett.

# **$^1\text{H}$ NMR Studies in the Regime of the Field-Induced Spin-Density Wave Phases of $(\text{TMTSF})_2\text{PF}_6$**

Brown, S.E., Univ. of California at Los Angeles, Physics and Astronomy

Clark, W.G., UCLA, Physics and Astronomy

Pieper, M., UCLA, Physics and Astronomy

Hillman, C., UCLA, Physics and Astronomy

Alavi, B., UCLA, Department of Physics and Astronomy

Lacerda, A., NHMFL/LANL

The layered molecular conductors of the Bechgaard salt family  $(\text{TMTSF})_2\text{X}$  are well-known for the variety of accessible ground states tuned by application of high pressure and magnetic field.<sup>1</sup> At ambient pressure,  $(\text{TMTSF})_2\text{PF}_6$  undergoes a metal-spin-density wave (SDW) transition at  $T=12.1$  K, while for pressures exceeding about 0.6 GPa the ground state is superconducting. Magnetic fields applied normal to the layers restore the insulating SDW state via a cascade of phase transitions. The intermediate phases are known as field-induced spin-density waves, and each is characterized by a quantized Hall plateau and quantization index  $n$ .

Here we present  $^1\text{H}$  spin lattice relaxation rate data in  $(\text{TMTSF})_2\text{PF}_6$  at pressures where the field-induced SDWs are accessible to temperatures below 1 K and magnetic fields ranging from 3.5 T to 18 T.<sup>3</sup> The experiments were carried out in two different magnets. The first measurements were in fields ranging from 10 to 18 T and confined to temperatures above 1.6 K, performed at the NHMFL in Los Alamos. More recently, we extended the measurements down to 0.8 K in fields up to 12.8 T at UCLA. The high pressure was produced using a standard clamp cell arrangement designed to minimize

signal contributions from protons outside the sample. In these experiments, signals were obtained up to 800 MHz in the pressure cell at the NHMFL.

In Figure 1, we show a summary of the relaxation rate data taken from the two experiments and evaluated by measuring the spin echo height after saturation. The peak in  $T_1^{-1}$  is the principal signature of the transition. By this method,  $T_{\text{FISDW}}$  was found to increase approximately linearly from a critical magnetic field  $H_c$  4 to 5 T. The results for  $T_{\text{FISDW}}$  are in good quantitative agreement with the findings of transport measurements at comparable magnetic fields.<sup>2</sup> The strength of the relaxation rate increases as the field increases, which is probably attributable to the increase of the zero-temperature gap parameter with magnetic field. That is,  $T_1^{-1} \sim \nu^{-1}$ , with  $\nu$  the coherent volume.<sup>4</sup>

**Acknowledgements.** This work was supported in part by the NSF under grant nos. DMR-9971530 (SB) and DMR-9705364 (WGC).

<sup>1</sup> Ishiguro, T. and Yamaji, K., *Organic superconductors* (Springer-Verlag, Berlin, 1990).

<sup>2</sup> Hannahs, S.T., *et al.*, Phys. Rev. Lett., **63**, 1988 (1989).

<sup>3</sup> Brown, S.E., *et al.*, J. Phys. IV Proceedings, **9**, Pr 10-187(1999).

<sup>4</sup> Virosztek, A. and Maki, K., Phys. Rev. B, **35**, 1954 (1987).

## **Measuring Properties of Materials in Pulsed Magnetic Fields with a Radio Frequency Tunnel Diode Oscillator**

Coffey, T., Clark Univ., Physics

Bayindir, Z., Clark Univ., Physics

DeCarolis, J., Clark Univ., Physics

Agosta, C.C., Clark Univ., Physics

Bennett, M., NHMFL, LANL

Tokumoto, M., ETL, Japan

We have developed a radio frequency measurement technique based on a tunnel diode oscillator (TDO) that is suitable for millisecond and longer pulsed magnetic fields. We have successfully used this technique to measure the penetration depth in a superconductor and Shubnikov-de Haas (SdH) oscillations (oscillations in resistivity) as a function of magnetic field in organic conductors. These experiments were done in the 60 T Long Pulse magnet at the NHMFL at Los Alamos. Similar experiments in the short pulsed field showed the feasibility of the technique in millisecond pulsed magnetic fields.

In the TDO system the sample is placed in the coil of a self resonant tank circuit. Measuring the frequency and the amplitude of the circuit oscillations gives information about the penetration depth, resistivity, or susceptibility of the sample. An advantage over traditional transport measurements, even for DC measurements, is that no leads need to be attached to the sample creating contact resistance or stressing the sample.

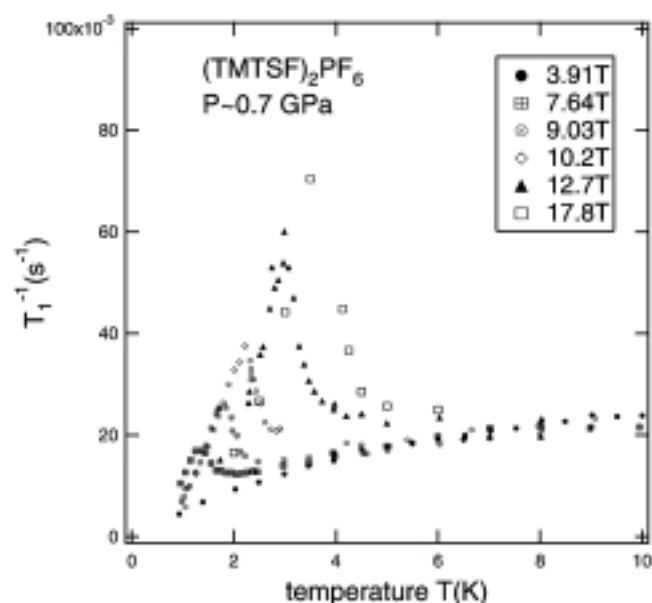


**Figure 1.**  $^1\text{H}$   $T_1^{-1}(T)$  at different magnetic fields in  $(\text{TMTSF})_2\text{PF}_6$  pressurized to  $P \sim 0.7$  GPa.

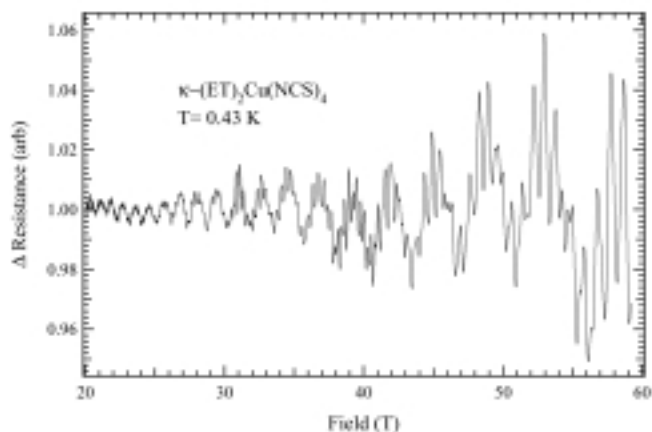


**Figure 1.** The Shubnikov de Haas effect in the organic conductor  $\kappa\text{-(ET)}_2\text{Cu(NCS)}_4$ .

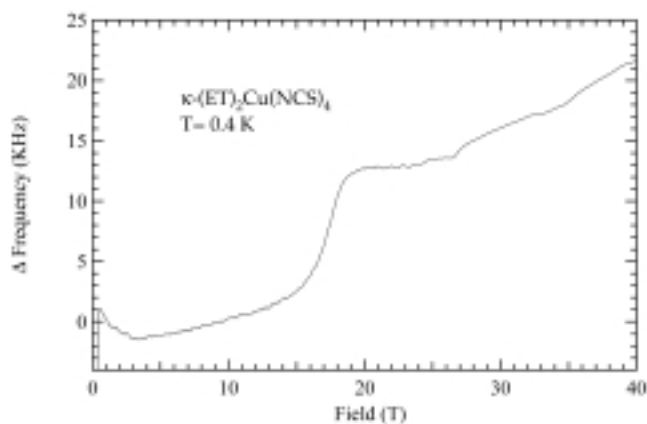


**Figure 2.** The superconducting transition in an organic conductor with the field near parallel to the conducting planes. The change in frequency is proportional to the penetration depth.

Two problems had to be overcome to use the standard TDO method in a pulsed magnetic field. The first problem is that the coil used in the tank circuit at the heart of the TDO generates a voltage due to the  $dB/dt$  of the magnet pulse and this voltage will push the diode off of its bias point during a pulse. The second problem was how to measure the frequency and amplitude rapidly during the magnet pulse. To solve the first problem we used a double counter wound sample coil. The coils are far enough apart that they do not couple well enough to cancel each other's inductance, but the global field of the pulse magnet will induce equal and opposite voltages on each coil. The sample however, only affects one coil. The result is that the filling factor of the sample is halved, the inductance is double that of a single coil, and the induced voltage on the double coil set from the global  $dB/dt$  is zero.

To solve the second problem we wanted to make an analog discriminator that could provide us with two voltages that were proportional to frequency and amplitude. We also wanted to use a fast digitizer to record the oscillations directly. The raw oscillations could then be analyzed using software at a later time to find the amplitude and frequency as a function of time. The method we chose for designing the analog discriminator came from a suggestion by Gil Clark (UCLA). The principle is

to split the signal into two parts and create a linear frequency dependent phase shift on one of the two signals. We used a simple LCR band pass filter tuned near the mixed down TDO frequency and with a bandwidth comparable to the total change we expected in the TDO frequency to provide the phase shift in one of the signals. With a lock-in amplifier we found the amplitude and phase between the two signals, which we converted into amplitude and frequency.

A sample of the data we collected is shown below using in the first case the digital and in the second case the analog measurement method. Figure 1 shows the SdH oscillations in the organic conductor  $\kappa\text{-(ET)}_2\text{Cu(NCS)}_4$  with the background divided out. Figure 2 shows the superconducting transition in the same compound with the conducting layers nearly parallel to the applied magnetic field. More details of this technique will be found in a publication submitted to the Review of Scientific Instruments with the same authors as this report.

## Angle Dependent Resonances in the Organic Superconductor $\kappa\text{-(ET)}_2\text{Cu(NCS)}_2$

Edwards, R.S., Univ. of Oxford, Physics  
 Schrama, J.M., Univ. of Oxford, Physics  
 Rzepniewski, E., Univ. of Oxford, Physics  
 Ardavan, A., Univ. of Oxford, Physics  
 Singleton, J., Univ. of Oxford, Physics  
 Kurmoo, M., Institut de Physique et Chimie des Matériaux de Strasbourg, (IPCMS), France

We have performed an angle dependent study of the millimeter-wave response of the organic charge-transfer salt  $\kappa\text{-(ET)}_2\text{Cu(NCS)}_2$ <sup>1</sup> using a unique rotating rectangular cavity system.<sup>2</sup> This is a well-studied superconductor, whose Fermi surface (FS) consists of a closed quasi two-dimensional (Q2D) section and two warped quasi one-dimensional (Q1D) sheets. Good quality crystals are available.

A crystal was placed inside a resonant rectangular cavity that provides a well-defined resonance at 71.2 GHz, with a quality factor when empty of about 1500. Our system enables us to rotate this cavity with respect to the applied magnetic field; the direction of the field with respect to the conducting planes of the sample can be changed without altering its electromagnetic environment. In traditional metals, radiation cannot penetrate the bulk of the metal, and only a measurement of the surface conductivity can be made. In the organic metals such as  $\kappa\text{-(ET)}_2\text{Cu(NCS)}_2$ , however, the very low interplane conductivity leads to an interplane skin-depth larger than the sample, and the millimeter-waves can penetrate the whole sample. We therefore measure the bulk interplane conductivity of the sample.



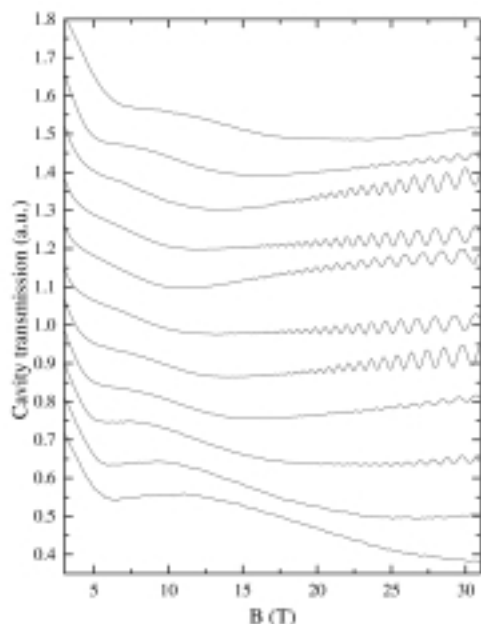


**Figure 1.** Millimeter-wave magneto-optics of  $\kappa\text{-(ET)}_2\text{Cu(NCS)}_2$ ; cavity transmission plotted against applied field for several different angles (from top,  $\theta = 60^\circ, 45^\circ, 30^\circ, 15^\circ, 0^\circ, -15^\circ, -30^\circ, -40^\circ, -45^\circ, -55^\circ, -60^\circ$ ). The sweeps have been normalized at 0 T and offset for clarity ( $T=1.4$  K).

Figure 1 shows the transmission of the cavity at different tilt angles for applied fields of up to 33 T. At low field a feature due to the superconductivity can be seen. At higher fields there is a broad resonance which moves in field as the cavity is rotated. Figure 2 shows the position in inverse field of this resonance as a function of rotation angle, fitted to  $\omega/B = A\cos(\theta - \theta_0)$ . A value of  $\theta_0 = 6^\circ \pm 1^\circ$  is found. For a cyclotron resonance<sup>3</sup> (CR) due to the closed Q2D section of the FS, an angle dependence of  $\omega/B = A\cos\theta$  is expected, i.e.  $\theta_0 = 0$ . It is also possible, however,

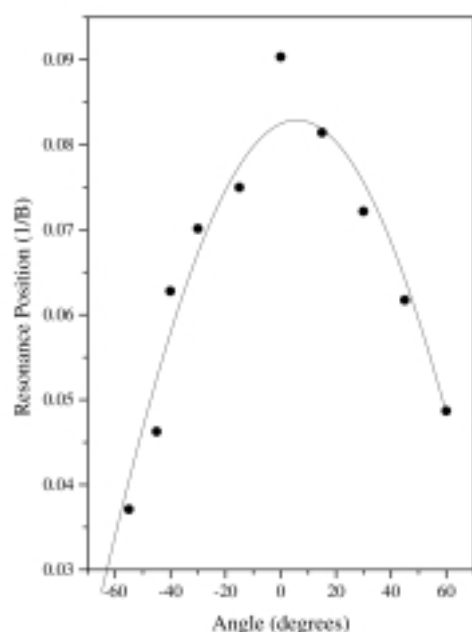


**Figure 2.** Position of the resonance observed in inverse field for different angles, fitted to  $\omega/B = A\cos(\theta - \theta_0)$ .

to see a resonance due to the warped Q1D FS sections, known as Fermi-surface Traversal Resonance (FTR).<sup>2</sup> To distinguish between the two effects it is necessary to repeat the measurement after changing the orientation of the sample inside the cavity. For a CR, the behavior of the resonance with tilt angle will not vary with orientation. If the resonance is an FTR, this behavior will vary with orientation in different ways depending on the warping components of the Q1D FS section.<sup>2</sup> For a warping component that is not purely inplane the value of  $\theta_0$  will change with orientation (see Reference 2 for more details). We have performed further experiments in Oxford for several different sample orientations. Results indicate that the resonance is an FTR. Preliminary analysis suggests that the Q1D section of the FS of  $\kappa\text{-(ET)}_2\text{Cu(NCS)}_2$  has two warping components, with warping vectors oriented at approximately  $30^\circ$  and  $-80^\circ$  to the interplane direction.<sup>4</sup> We see no effect from the Q2D FS section.

<sup>1</sup> See e.g. Ishiguro, T., *et al.*, "Organic Superconductors," Springer Verlag, Berlin (1990).

<sup>2</sup> Ardavan, A., *et al.*, Phys. Rev. Lett., **81**, 713 (1998).

<sup>3</sup> Blundell, S.J., *et al.*, Phys. Rev. B, **55**, R6129 (1997).

<sup>4</sup> Schrama, J.M., *et al.*, to be published.

## Anomalous Low Temperature Conductivity in $(\text{TMTSF})_2\text{PF}_6$

Han, S.Y., NHMFL/FSU, Physics

Brooks, J.S., NHMFL/FSU, Physics

Rutel, I.B., NHMFL/FSU, Physics

Anzai, H., Himeji Institute of Technology, Japan

$(\text{TMTSF})_2\text{PF}_6$  experiences a characteristic jump in the resistance at  $T_{\text{SDW}} = 12$  K due to the opening of a SDW gap and shows a clear activated behavior,  $R(T) = R_0 \exp(-\Delta/k_B T)$ , with an activation energy,  $\Delta = 16$  to 23 K.<sup>1</sup> The growth in the resistance below 3 K, however, actually deviates drastically from the higher temperature activated pattern. Although this behavior has been seen in many measurements,<sup>2</sup> it has been attributed as an experimental artifact. A reason is because experimental artifacts such as heating, non-linear effects, or instrumental effect can easily cause an apparent saturation of the low temperature resistance since the resistance in this low temperature range is very large.

We carefully examined this low temperature saturated behavior in resistance with DC resistance measurements in the mK regime. Measurements were made on five  $(\text{TMTSF})_2\text{PF}_6$  samples and one  $(\text{TMTSF})_2\text{AsF}_6$  samples. Four terminal DC resistance measurements were carried out along the c and a axis of the samples. A high resolution nano-voltmeter was used for measurements in a configuration where the DC current was periodically switched to cancel residual thermal emf signals in the circuitry. Ohmic behavior was assured by measuring I-V curves in all cases. Nominally, currents of order 1 nA gave reliable ohmic behavior.

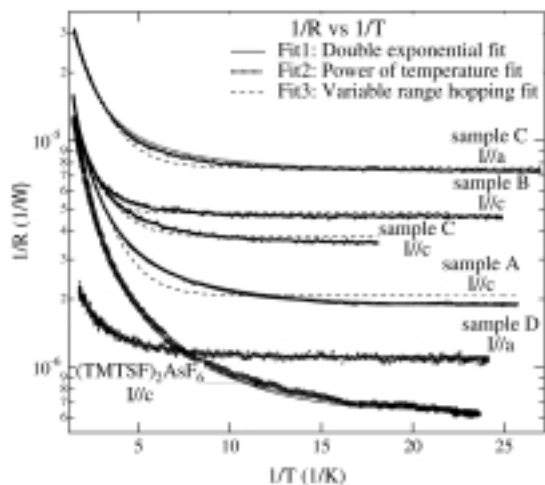


**Figure 1.** The inverse resistance of (TMTSF)<sub>2</sub>PF<sub>6</sub> and (TMTSF)<sub>2</sub>AsF<sub>6</sub> and numerical fittings are plotted as a function of inverse temperature.

A summary of our low temperature measurements at zero magnetic field are shown in Figure 1. The conductivity, which is clearly activated at higher temperatures, becomes only weakly temperature dependent in the low temperature limit. We note that since care was taken to avoid the effects of heating and non-ohmic behavior, we believe that the observed low temperature behavior is accurate. The best description of the data is given by a double exponential fit, according to  $\sigma(T) = \sigma_1 \exp(-T_{01}/T) + \sigma_2 \exp(-T_{02}/T)$  where values of the activation energies for all cases studied fall into the general range  $T_{01}$  0.3–0.5 K,  $T_{02}$  1.5–3 K. The double exponential form of conductivity provides for additional, lower energy scales, which account for the weak decrease in  $\sigma(T)$  below 3 K. An almost equally good fit may be obtained by a power law ( $T^\alpha$ ), which would be characteristic of anomalous metallic and/or insulating behavior. It is clear, however, that a variable range hopping ( $\exp(-T_0/T)^\alpha$ ) form cannot account for the observed behavior. In Figure 2,

the magnetoresistance for selected directions of magnetic fields are shown. We observe unusual negative magnetoresistance at lower fields with the resistance at zero field is 13 to 18% higher than minimum magnetoresistance. This behavior is getting weaker as temperature increases and disappears above 1 K. Anomalous negative magnetoresistance has been observed in samples from different growers and in different facilities by different observers. The exact nature of the negative magnetoresistance is not clear yet and more detailed investigation is needed. The existence of magnetoresistance in this temperature range, however, by itself supports the existence of conduction mechanism.

Based on the observed temperature dependence, we may consider the origin of the low temperature behavior of  $\sigma(T)$ . Since it does not follow any characteristic hopping or power law behavior, and since the transport is ohmic, it is unlikely to be the result of collective mode (Frolich) motion. Given the above discussion, the most likely origin of the anomalous conductivity is the continued improvement of the nesting condition. Following Brooks *et al.*<sup>3</sup>, we note that below 3 K the reconstructed, nested Fermi surface retains its overall topology, but that the remaining small pockets become smaller as the nesting condition improves over more of the remaining Fermi surface. Clearly, with a resistivity of M -cm or more, this involves very small pockets and very small changes. Nevertheless, the effects are very significant in the observed transport behavior, including both the attenuation of the quantum oscillations, and also the temperature dependence of the conductivity.

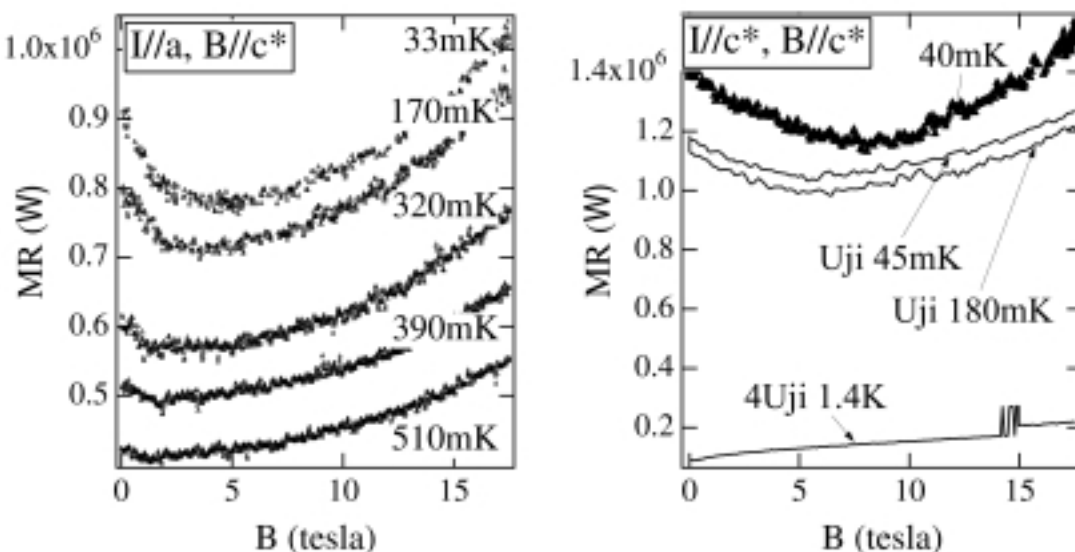


**Figure 2.** The magnetoresistance of (TMTSF)<sub>2</sub>PF<sub>6</sub> is plotted as a function of magnetic field. The left side of the figure is a case with the current direction parallel to a axis at different temperatures and the right side is a case with the current direction parallel to c axis. For the comparison, we also plot data taken by S. Uji along with our data scaled to Uji's data. The magnetic field is fixed at the direction parallel to c axis in all data.

<sup>1</sup> Wosnitza, J., *Fermi Surfaces of Low-Dimensional Organic Metals and Superconductors*, (Springer Verlag, Berlin-Heidelberg, 1996).

<sup>2</sup> Uji, S., *et al.*, Phys. Rev. B, **55**, 12446 (1997).

<sup>3</sup> Brooks, J.S., *et al.*, Phys. Rev. B, **59**, 503 (1999)

# Zeeman Effect on de Haas-van Alphen Oscillations in a 2D Magnetic Breakdown System

Han, S.Y., NHMFL

Brooks, J.S., NHMFL/FSU, Physics

Kim, Ju. H., Univ. of North Dakota, Physics

We use a quantum mechanical model to compute magnetic quantum oscillations in two dimensional magnetic breakdown systems. A tight binding model was derived from the actual crystal structure and atomic orbital of  $\alpha$ -(ET)<sub>2</sub>KHg(SCN)<sub>4</sub> according to the extended Hückel prescription. Four bands and seven different transfer integrals replicate the real system. An extra magnetic symmetry generates a Hofstadter<sup>1</sup> type energy spectrum by taking magnetic fields satisfies the condition, the ratio of the magnetic flux per unit cell to the flux quantum ( $\phi/\phi_0$ ) becomes a ratio of integers  $p/q$ . From the energy spectrum the field dependent magnetization can be calculated following the standard procedure<sup>2</sup>. As a result, dHvA oscillations with breakdown effect and  $f_{\beta-\alpha}$  appeared naturally as an outcome.<sup>3</sup> In this report we present a new result that was obtained by including the non-interacting spin effect in the previously described calculation. Our quantum mechanical results are also compared with the standard Lifshitz-Kosevich (LK) formula.<sup>4</sup>

When non-interacting spins are considered, spin states are orthogonal to other eigen states and spin terms only appear in the diagonal elements of the matrix with the matrix size doubled from the spinless Hamiltonian. The Hamiltonian can be represented by:  $H = H_0 + H_S$ , and  $H_S = g\sigma\mu_B B/2$ , where  $\sigma$  is  $\pm 1$  and  $g$  is the spin splitting factor close to 2. The spin degeneracy

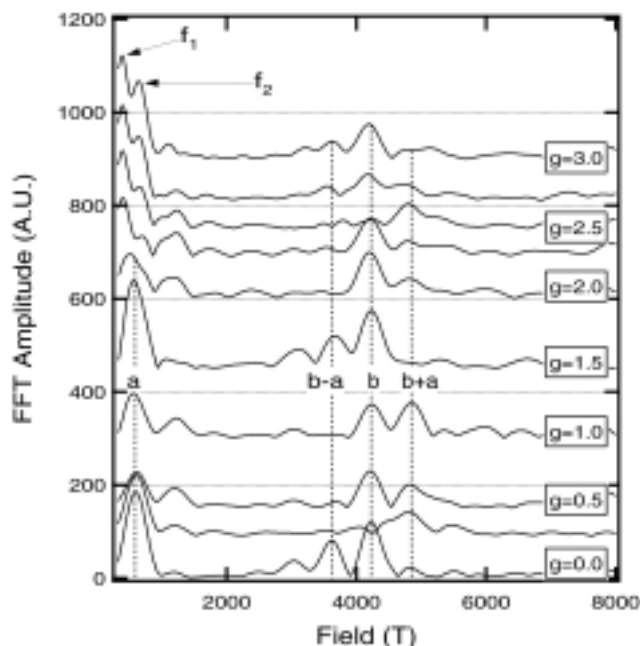


**Figure 1.** The FFT spectrums for  $g$  between 0 to 3. Curves are offset in proportion to  $g$ .

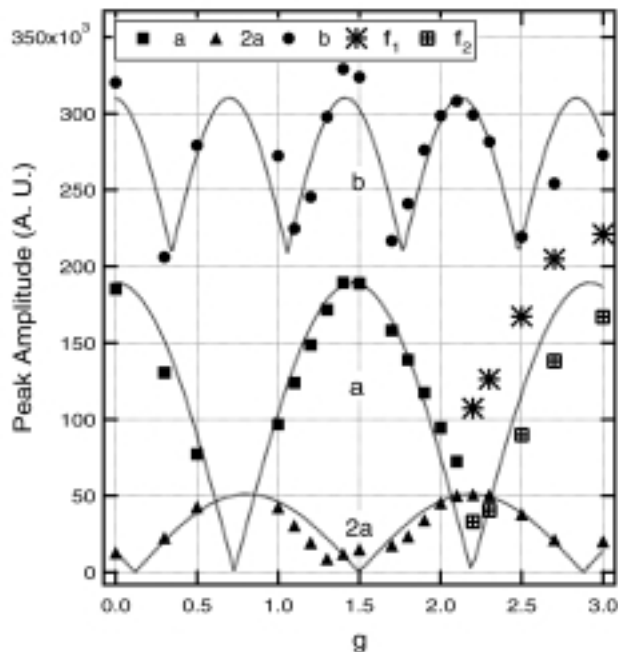


**Figure 2.** The FFT amplitudes vs.  $g$  and the LK spin term,  $R_S$ . The  $f_1$  and  $f_2$  are new frequencies that split from  $f_\alpha$  for  $g > 2.1$ .

is lifted and energy levels linearly split to up and down spin levels. In LK formula the phase difference coming from the linear spin splitting causes a damping factor,  $R_S$  in magnetic oscillations, where  $R_S$  is proportional to  $\cos(1/2\pi g m^*)$ . We calculate the magnetization for several  $g$  values at a finite temperature close to zero. The dHvA oscillations are Fourier transformed (FFT) in Figure 1. The amplitude of each peak periodically oscillates as a function of  $g$ .

In Figure 2, peak amplitudes as a function of  $g$  are plotted and numerically fitted to the absolute value of  $R_S$ . The cosine behavior expected from the LK is confirmed even in these high fields with the existence of the Hofstadter energy substructures. From the LK fitting we also estimated the effective masses. The estimates of effective masses are  $1.37 m_e$  for  $m^*_{s_\alpha}$  and  $2.85 m_e$  for  $m^*_{s_\beta}$ . These are close in value to those from the temperature fitting. Another important aspect we obtain from the  $g$  dependent FFT result is the splitting of the fundamental frequency at high  $g$  values. The fundamental frequency,  $f_\alpha$  (599 T) splits into two new frequencies,  $f_1$  (382 T) and  $f_2$  (626 T). We find that the LK description of the spin damping holds even in systems with a complex energy spectrum and in extremely high magnetic fields.

**Acknowledgements:** This research was supported by NSF-DMR 99-71474 and 95-10427 (JSB). The NHMFL is supported through a Cooperative Agreement between the NSF through NSF-DMR-95-27035 and the State of Florida.

<sup>1</sup> Hofstadter, D.R., Phys. Rev. B, **14**, 2239 (1976).

<sup>2</sup> Landau, L.D. and Lifshitz, E.M., *Statistical Physics 3rd edition*. (Course of Theoretical Physics. Vol. 5., 1976).

<sup>3</sup> Kim, Ju. H., *et al.*, Phys. Rev. B, **60**, 3213 (1999).

<sup>4</sup> Lifshitz, I.M. and Kosevich, A.M., Zh. eksp. teor. fiz., **29**, 730 (1955).

## Quantum Oscillations in the Charge-Density Wave Compound NSe<sub>3</sub> in Strong Magnetic Fields

Harrison, N., LANL

Balicas, L., Venezuelan Institute for Scientific Research;  
NHMFL/FSU, Physics

Brooks, J.S., NHMFL/FSU, Physics

Mielke, C.H., LANL

Sarrao, J., LANL

Fisk, Z., NHMFL/FSU, Physics

This year we set out to study quantum oscillatory effects in some well known charge-density wave compounds. This was partly motivated by similar studies made on certain organic conductors based on the BEDT-TTF molecule that had recently been suggested to possess a charge-density wave.<sup>1,2</sup>

Our interest turned to NbSe<sub>3</sub> because its quantum oscillations have a similar structure<sup>3</sup> to those in the low magnetic field phase of  $\alpha$ -(BEDT-TTF)<sub>2</sub>KHg(SCN)<sub>4</sub>: *i.e.* there is a pronounced second harmonic content in this material that cannot be explained by Zeeman splitting of the Landau levels in a magnetic field.<sup>2</sup> By performing transport measurements at various orientations of the magnetic field in NbSe<sub>3</sub> in fields up to 31 T, we were able to show that the apparent splitting of the oscillations in this material definitely cannot be attributed to the Zeeman splitting effect.<sup>4</sup> The alternative explanation is that an enhanced second harmonic contribution to the quantum oscillations originates from interference effects between the oscillations of the chemical potential and the charge-density wave.<sup>2</sup> Some examples of the magnetoresistance of NbSe<sub>3</sub> are shown in Figure. 1.

Further studies were pursued in pulsed magnetic fields in order to find how high in temperature quantum oscillations could be observed. Some structure was still observable in field of ~60

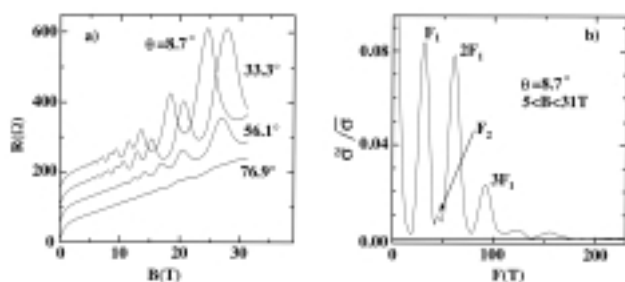


**Figure 1.** (a) Examples of the magnetoresistance of NbSe<sub>3</sub> measured at several orientations of the magnetic field. (b) A Fourier transform, revealing two fundamental frequencies.

T up to ~50 K, although this is still below the lower charge-density wave transition temperature in NbSe<sub>3</sub> of ~59 K.

<sup>1</sup> McKenzie, R.H., cond-mat/9706235.

<sup>2</sup> Harrison, N., Phys. Rev. Lett., **83**, 1395 (1999).

<sup>3</sup> Monceau, P., Solid State Commun., **24**, 331 (1977).

<sup>4</sup> Harrison, N., under review.

## The Thermodynamic Properties of $\alpha$ -(BEDT-TTF)<sub>2</sub>KHg(SCN)<sub>4</sub>

Harrison, N., LANL

Balicas, L., Venezuelan Institute for Scientific Research;  
NHMFL/FSU, Physics

Brooks, J.S., NHMFL/FSU, Physics

Mielke, C.H., LANL

The organic density wave material  $\alpha$ -(BEDT-TTF)<sub>2</sub>KHg(SCN)<sub>4</sub> has been the subject of many experimental investigations for at least 10 years, and is still largely not understood. While this material was originally considered to possess a spin-density wave,<sup>1</sup> from the thermodynamic perspective, the phase diagram is completely unlike that to be expected for a spin-density wave; rather it is more like that of a charge-density wave.<sup>2,3</sup> Until some measurement is made that can definitively prove either case, this will continue to remain a topic of hot debate.

We recently performed numerous measurements of the field orientation dependence of the quantum oscillations both in pulsed magnetic field and in static magnetic fields in Tallahassee. One of our findings has been that the product of the effective mass with the electron g factor is independent of field, irrespective of the phase transitions. What this implies is that electron-electron interactions are either irrelevant or do not change across the phase diagram.

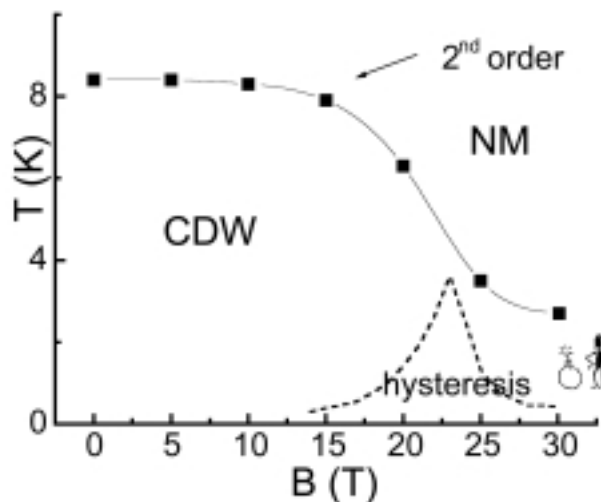


**Figure 1.** The thermodynamic phase diagram of  $\alpha$ -(BEDT-TTF)<sub>2</sub>KHg(SCN)<sub>4</sub>.



We also measured hysteresis effects in the quantum oscillations within the high magnetic field phase. The nature of the high magnetic field phase is still far from understood. It could be an incommensurate charge-density wave with a spatially varying order parameter, although the magnetic and transport properties are very much unlike those in normal charge density wave systems. This phase could then be considered analogous to the Fulde-Ferrel phase anticipated to exist in type II superconductors with suppressed orbital effects. A snapshot of the phase diagram obtained from thermodynamic magnetic torque measurements is shown in Figure 1.

<sup>1</sup> Sasaki, T., *et al.*, *Synth. Met.*

<sup>2</sup> McKenzie, R.H., *cond-mat/9706235*

<sup>3</sup> Harrison, N., *Phys. Rev. Lett.* **83**, 1395 (1999).

## Angle Dependent Magnetization within the Superconducting State of $\kappa$ -(ET)<sub>2</sub>Cu(NCS)<sub>2</sub>

Hill, S., Montana State Univ., Physics  
Mola, M., Montana State Univ., Physics  
Brooks, J.S., NHMFL/FSU, Physics  
Qualls, J.S., NHMFL/FSU, Physics

There has been considerable recent interest in the superconducting states of several highly anisotropic organic superconductors due to the possibility that the pairing mechanism may be unconventional, i.e. non-singlet s-wave. Members of the  $\kappa$ -phase BEDT-TTF (ET for short) charge transfer salts have, perhaps, attracted most attention.<sup>1</sup> Measurements in high magnetic fields have played an important role in this debate, particularly those in which the field orientation may be varied with respect to the sample. A wide range of novel phenomena have been predicted to occur in unconventional superconductors subjected to a magnetic field,<sup>1</sup> e.g. re-entrant superconductivity in triplet superconductors or, in the case of singlet pairing, a transition to a non-uniform superconducting state (Fulde, Ferrell, Larkin and Ovchinnikov) upon reaching the Pauli paramagnetic limit. Furthermore, there is immense interest in the structure and dynamics of supercurrent vortices within the mixed state of highly type-II superconductors;<sup>2</sup> indeed, an understanding of vortex dynamics has important technological implications since this is the predominant mechanism for dissipation. Several recent experiments have addressed these issues. To our knowledge, however, angle dependent magneto-thermodynamic measurements on clean organic superconductors, and at ultra-low temperatures and high magnetic fields, have been lacking.

High purity organic charge transfer salts provide possibly the best systems for studying unconventional forms of superconductivity because their upper critical fields are readily accessible using continuously powered magnets (< 30 T); their underlying electronic structures are well known; and, due to the virtual absence of defects, their intrinsic electronic

properties dominate most low-temperature measurements. Ultra-low temperatures are important in the context of studying vortex structure/dynamics due to the suppression of thermal fluctuation effects. We have conducted angle dependent magnetic torque measurements on two samples of the organic superconductor  $\kappa$ -(ET)<sub>2</sub>Cu(NCS)<sub>2</sub> in fields to 20 T and at temperatures in the range from 25 mK to 600 mK. The torque measurements were performed using a cantilever magnetometer mounted on a single axis rotator. The field was rotated in a plane perpendicular to the samples' highly conducting bc-planes.

Although the results of this work are too recent (late Dec. 1999) to provide a complete analysis and discussion, we nevertheless attempt to summarize our preliminary findings. We see no evidence for any critical phenomena that could be attributed either to a change in the symmetry of the pairing, or to a transition to a non-uniform superconducting state. We observe, however, regular saw-tooth oscillations in the magnetization below 200 mK, and at fields below the irreversibility line ( $H_{irr}$ ), that we associate with changes in the vortex structure. Indeed, these oscillations exhibit a distinct temperature- and angle-dependent cut-off field,  $H_c < H_{irr}$ , above which the oscillations cease. This may be indicative of a first-order (probably 2D) vortex melting transition.

<sup>1</sup> See e.g. Zuo, F., *et al.*, *Phys. Rev. B*, **61**, 750 (2000); and references therein.

<sup>2</sup> See e.g. Cornaglia, P.S., *et al.*, *Phys. Rev. B*, **61**, 784 (2000); and references therein.

## Mapping of the Quantum Hall Regime in $\alpha$ -(BEDT-TTF)<sub>2</sub>MHg(SCN)<sub>4</sub> (M=K, Tl) Organic Conductors

Honold, M.M., Univ. of Oxford, Physics  
Nam, M.-S., Univ. of Oxford, Physics  
Singleton, J., Univ. of Oxford, Physics  
Yaguchi, H., Univ. of Oxford, Physics  
Harrison, N., LANL  
Mielke, C.H., LANL  
Kartsovnik, M.V., Walther-Meissner-Institut, Garching  
Kushch, N.D., ICPR, RAS, Chernogolovka  
Kurmoo, M., Institut de Physique et Chimie des Matériaux de Strasbourg (IPCMS), France  
Day, P., Royal Institution, London

The high magnetic field region of the quasi-two-dimensional organic conductors  $\alpha$ -(BEDT-TTF)<sub>2</sub>MHg(SCN)<sub>4</sub> (M=K, Tl) has recently attracted a lot of interest due to the observation of unusual magnetotransport effects such as the phase inversion of the oscillations in the interplane magnetoresistance,<sup>1,2</sup> the suggestion of the occurrence of the bulk quantum Hall effect<sup>3</sup> and the proposal of new low-temperature, high-field phase.<sup>4</sup> Comprehensive pulsed magnetic field measurements of the interplane magnetoresistance and Hall potential oscillations as a function of magnetic field, temperature, rotation angle, sweep

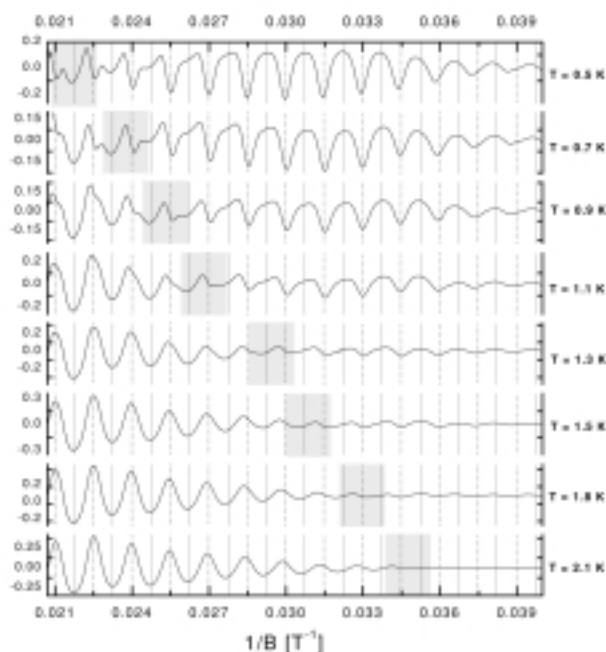


**Figure 1.** The oscillatory part of  $\rho_{zz}$  within the high-field region at  $\theta = 0^\circ$  for a variety of temperatures. The dotted lines indicate integer filling factors, the solid lines odd half-integer filling factors. The shaded regions denote a phase change of  $\Phi = \pi$ .

rate, sample quality and the anion of the charge-transfer salt suggest that these observations can be interpreted in a consistent manner.

Our results are consistent with the establishment of the quantum Hall effect above the magnetoresistive kink transition and its destruction at high magnetic fields. An increase in rotation angle allows the quantum Hall effect to persist to higher fields. The inversion of the oscillation phase of  $\rho_{zz}$  is interpreted as the short-circuiting of interplane current paths by highly conducting edge states at the sample surface. The effect of this surface metal on the longitudinal transport has already been demonstrated in semiconductor superlattices that exhibit the

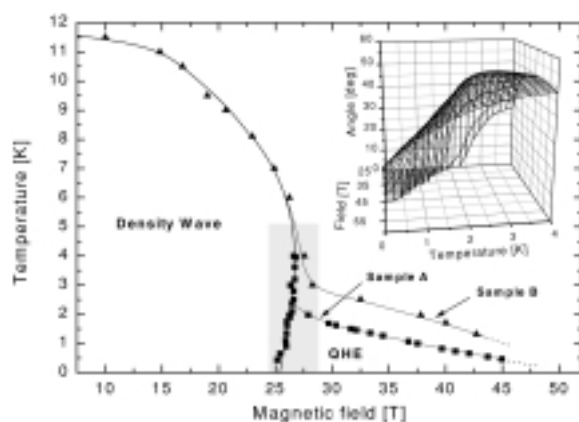


**Figure 2.** Diagram, mapping the region of phase space over which the oscillation phase of  $\rho_{zz}$  is inverted; this region can be associated with the presence of the quantum Hall effect. The shaded area denotes the transition region between the low temperature-low field density wave and the high-field regime. Inset: three-dimensional diagram with the rotation angle plotted along the vertical axis.

quantum Hall effect.<sup>5</sup> The inversion of the oscillation phase of  $\rho_{zz}$  (Figure 1) is found to be directly related to the quality of the sample and is suggested to be an intrinsic property of  $\alpha$ -(BEDT-TTF)<sub>2</sub>MHg(SCN)<sub>4</sub> (M=K, Tl). A detailed mapping of the phase-inverted region indicates that its boundaries agree qualitatively with those of the recently proposed low temperature-high field state (Figure 2). The inset to Figure 2 shows a surface plot of the boundary with rotation angle plotted along the vertical axis. The T- $\theta$  plane at B~25 T corresponds to the boundary of the low-field density wave state. The region between this plane and the plotted surface marks the regime where the “phase inversion effect” occurs.

<sup>1</sup> Honold, M.M., *et al.*, J. Phys. Condens. Matt., **9**, L533 (1997).

<sup>2</sup> Hill, S., *et al.*, Phys. Rev. B, **55**, R4891 (1997).

<sup>3</sup> Harrison, N., *et al.*, Phys. Rev. Lett., **77**, 1576 (1996).

<sup>4</sup> Kartsovnik, M.V., *et al.*, Synth. Met., **86**, 1933 (1997).

<sup>5</sup> Druist, D.P., *et al.*, Phys. Rev. Lett., **80**, 365 (1998).

## Multifrequency, High Field EPR Study of Low-Dimensional Radical Ion Salts

IHRP

Krzystek, J., NHMFL

Sienkiewicz, A., Institute of Physics, Polish Academy of Sciences

Von Schütz, J.U., Univ. of Stuttgart, Germany, Physics Institute

Radical ion salts of the series Me(2,5-DMDCNQI)<sub>2</sub> where Me = Li<sup>+</sup>, ..., Ag<sup>+</sup>; 2,5-DMDCNQI = 2,5-dimethyldicyanoquinonediimine, have attracted considerable attention in recent years due to their fascinating electrical and magnetic properties. These properties strongly depend on the metal ion involved, with the Cu salt displaying very high conductivity in a broad temperature range.<sup>1</sup>

EPR has been one of the most successful methods to investigate the magnetic properties of the DCNQI salts. In particular, through the measurements of relaxation rates and establishing the relaxation mechanism, it allowed to correlate the magnetic and electrical properties.<sup>2</sup> Previous EPR experiments were performed mostly at X-band. In the present study we extended the EPR spectroscopy to much higher frequencies and fields. In doing so, we intended to:

- (i) Follow the relaxation properties that allow one to predict the mobility. Of the greatest interest was the transition from the mobility-determined to exchange-determined dynamics, in particular in the situation when the conductivity breaks down due to the localization of charge density waves while the magnetic susceptibility remains constant. Earlier studies limited the observable correlation times to  $\tau > 10^{-10}$  s. With high frequencies, shorter correlation times can be followed;
- (ii) Test existing models of field-induced spin-orbit coupling (SOC) contributions through the field dependence of the EPR linewidth;

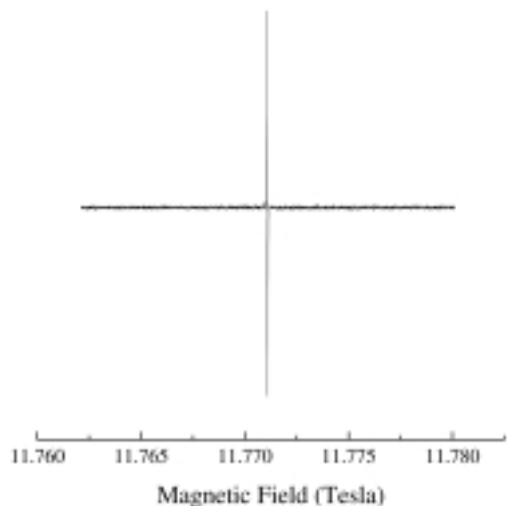


**Figure 1.** Lithium phthalocyanine single crystal EPR spectrum at 330 GHz and 273 K. This is the narrowest signal recorded at 12 T;  $\Delta B_{pp} = 20 \mu\text{T}$  (magnet homogeneity limit).

- (iii) Observe effects around the possible Peierls transition of the kind recently reported;<sup>3</sup>
- (iv) Approach the “isolated” molecular g-tensor via the angle dependency of the line positions at low temperatures.

We obtained preliminary results of high field EPR experiments in a broad frequency (110 to 440 GHz), and temperature (4.2 to 300 K) range on a single crystal of  $\text{Li}(2,5\text{-DMDCNQI})_2$ . In particular, an increase of linewidth with increasing frequency can be attributed to a field-induced SOC contribution, and an appearance of well-resolved extra lines below 35 K can be correlated with a Peierls-type phase transition and/or slowing down the exchange.

Additionally, high field EPR results on a semiconducting lithium phthalocyanine complex single crystal characterized by very small linewidths<sup>4</sup> were obtained.

- <sup>1</sup> Mori, T., *et al.*, Phys. Rev. B, **38**, 5913 (1988).
- <sup>2</sup> Krebs, M., *et al.*, Synth. Metals, **64**, 187 (1994).
- <sup>3</sup> Tomic, S., *et al.*, Europhys. Lett., **38**, 219 (1997).
- <sup>4</sup> Wachtel, H., *et al.*, Synth. Metals, **61**, 139 (1993).

## Kappa Phase Organic Superconductors with In-Plane Tilted Magnetic Field ( $H \parallel ac$ )

Mielke, C.H., NHMFL/LANL  
 Harrison, N., NHMFL/LANL  
 Montgomery, L.K., Indiana Univ., Chemistry

The organic superconductors  $\kappa\text{-(BEDT-TTF)}_2(\text{NCS})_2$  and  $\kappa\text{-(BEDT-TTF)}_2 \text{Cu}[\text{N}(\text{CN})_2]\text{Br}$  were studied at a tilted magnetic field with the  $ac$  planes aligned parallel to the applied magnetic field. The magnetoresistance was measured in pulsed

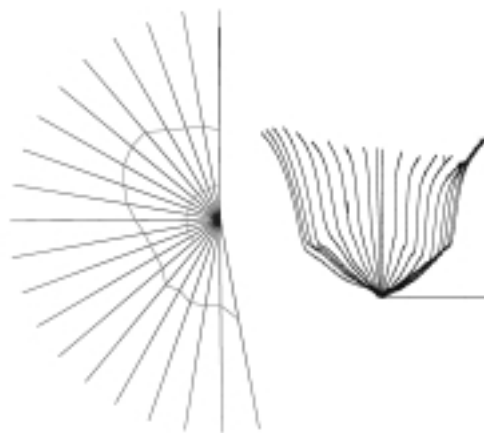


**Figure 1.** A three-dimensional view of the  $\kappa\text{-(BEDT-TTF)}_2(\text{NCS})_2$  data. The left plot shows an above view, outlining a magnetoresistance contour. The right hand view shows the data in an  $xy$  perspective.

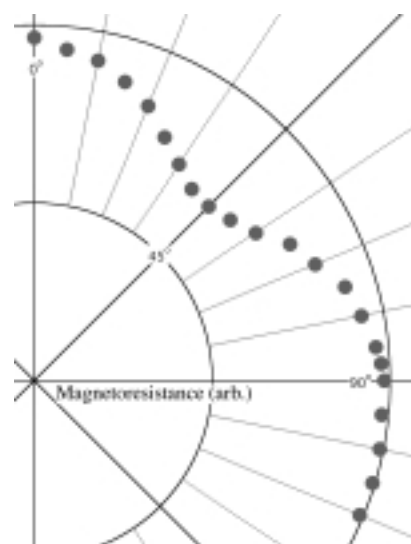


**Figure 2.** A polar plot of the magnetoresistance vs. relative angle for  $\kappa\text{-(BEDT-TTF)}_2 \text{Cu}[\text{N}(\text{CN})_2]\text{Br}$ . The polar axes are magnetoresistance vs. magnetic field at various angles with respect to applied field.

magnetic fields at  $T \sim 0.5 \text{ K}$ , at several angles in the compounds, rf lock-in techniques were used. A slight misalignment of the  $\kappa\text{-(BEDT-TTF)}_2 \text{Cu}(\text{NCS})_2$  was estimated to be  $1/2$  of a degree with respect to the  $b^*$  axis and the applied field. Figure 1 shows a three-dimensional polar plot of the data in two perspectives. The axes are magnetoresistance ( $x$ ), magnetic field ( $y$ ), and angle ( $\theta$ ). The left-hand perspective is a polar perspective, with the  $y$  axis out of the page. A contour line connects all of the traces at a constant magnetoresistance. Although these results are preliminary the contour shows only basic symmetry (two fold).

The  $\kappa\text{-(BEDT-TTF)}_2 \text{Cu}[\text{N}(\text{CN})_2]\text{Br}$  sample was studied in a similar fashion as just described. The sub  $H_{c2}$  magnetoresistance plots (at constant field vs. angle) were non-descriptive, however, the magnetoresistance above  $H_{c2}$  shows interesting symmetry. Figure 2 shows a polar plot of the magnetoresistance taken at 39 T.



## Josephson Plasma Resonance and Vortex Structure/Dynamics in Organic Superconductors

Mola, M., Montana State Univ., Physics

Hill, S., Montana State Univ., Physics

Brooks, J.S., NHMFL/FSU, Physics

Qualls, J.S., NHMFL/FSU, Physics

Ward, B.H., NHMFL/FSU, Physics

In highly anisotropic type-II superconductors, e.g. the high- $T_c$  cuprates and the quasi-two-dimensional (Q2D) organics, it has been well documented that a collective plasma mode—associated with the weak Josephson coupling between the layers—may lie at frequencies well below the superconducting gap. This mode is expected to produce a pronounced peak in the optical conductivity for currents perpendicular to the layers ( $\sigma_c$ ). Recently, it has been shown both experimentally<sup>1</sup> and theoretically<sup>2</sup> that this mode is extremely sensitive to the underlying vortex structure/dynamics within the mixed state. This is easily understood as being due to the dependence of the Josephson plasma frequency ( $\omega_p$ ) on the maximum interlayer Josephson current ( $J_m$ ), i.e.  $\omega_p^2 \propto J_m$ ; in turn,  $J_m$  depends on the inter-layer tunneling probability which, of course, depends on the arrangement of the vortices in adjacent layers.

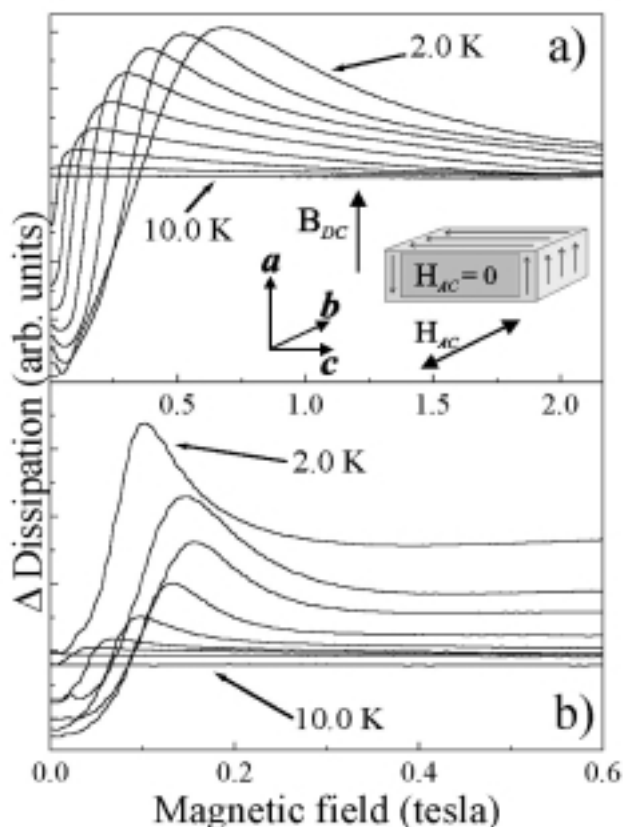


**Figure 1.** Temperature and field dependence of the JPR (dissipation maximum) in  $\kappa$ -(ET)<sub>2</sub>Cu(NCS)<sub>2</sub> at two frequencies: a) 76 GHz and b) 111 GHz. The temperatures are from 2 K to 10 K in increments of 1 K.

Through measurements of the Josephson Plasma Resonance (JPR), we have been able to probe the vortex structure/dynamics of several members of the highly anisotropic  $\kappa$ -phase BEDT-TTF (ET for short) based organic superconductors.<sup>3</sup> We find a different field/frequency behavior of the JPR, as compared to the high- $T_c$  materials, which may be attributed to the high quality of these samples. Indeed, the exponential relationship between  $\omega_p$  and the applied magnetic field strength,  $B$ , has been predicted for clean superconducting systems.<sup>2</sup> Furthermore, through measurements over a wide frequency range (28 to 153 GHz), we are able to access a large portion of the superconducting phase diagram, as shown in Figure 1, where a crossover in the temperature dependence of the JPR can be seen at low fields (Figure 1b); this is indicative of a transition in the vortex structure below  $\sim 4$  K.

<sup>1</sup> See e.g., Shibauchi, T., *et al.*, Phys. Rev. Lett., **83**, 1010 (1999); and references therein.

<sup>2</sup> Bulaevskii, L.N., *et al.*, Phys. Rev. Lett., **74**, 801 (1995).

<sup>3</sup> Mola, M., *et al.*, submitted to Phys. Rev. B (2000).

## Magnetotransport Measurement of Metallic Polyacetylene

Park, Y.W., Seoul National Univ., Physics, Korea/NHMFL

Suh, D.-S., Seoul National Univ., Physics, Korea

In the doped polyacetylene system, even though the conductivity value at room temperature was comparable to that of metal, the temperature dependence had shown the negative temperature coefficient of resistivity in wide range of temperature for the dopant such as iodine, AsF<sub>5</sub>, FeCl<sub>3</sub>, and ClO<sub>4</sub><sup>-</sup>. Recent discovery of metallic temperature dependence of resistivity for the ClO<sub>4</sub><sup>-</sup> doped polyacetylene<sup>1</sup> enables us to study the intrinsic metallic property of doped polyacetylene in a macroscopic film. Since the ClO<sub>4</sub><sup>-</sup> doped polyacetylene film is extremely sensitive to oxygen contamination as well as to aging, however, special care is necessary to minimize such external contamination factors.

In this experiment, we have investigated the magnetoresistance (MR) of ClO<sub>4</sub><sup>-</sup> doped polyacetylene film with relatively high room temperature conductivity. Figure 1 shows the temperature dependence of resistivity for various samples normalized by the room temperature value. Among the numerous data, the lowest resistivity ratio is achieved as  $\rho(1.2\text{K})/\rho(300\text{K})=1.04$  with the resistance minimum at  $T=150$  K,  $\rho(150\text{K})/\rho(300\text{K})=0.9$ . Although it does not show the metallic temperature dependence down to low temperature region, only 4% increase of resistance at  $T = 1.2$  K is observed in the perchlorate(ClO<sub>4</sub><sup>-</sup>) doped polyacetylene where Fe(ClO<sub>4</sub>)<sub>3</sub> was used for the ClO<sub>4</sub><sup>-</sup> doping. All of the other dopants including Cu(ClO<sub>4</sub>)<sub>2</sub> for the ClO<sub>4</sub><sup>-</sup> doping didn't show such low resistance increment at all.

The MR for the sample with the lowest  $\rho(1.2\text{K})/\rho(300\text{K})$  value is plotted in Figure 2. The characteristics of the MR data can be summarized as following: (1) Both longitudinal and transverse MR are negative. (2) The transverse MR is approximately twice as big as the longitudinal one in its magnitude. (3) Longitudinal



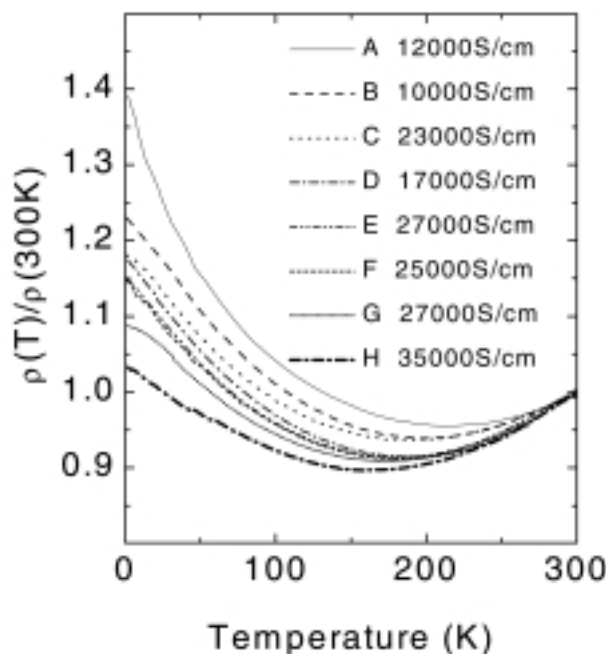


**Figure 1.** Temperature dependence of resistivity of  $\text{ClO}_4^-$  doped polyacetylene films.

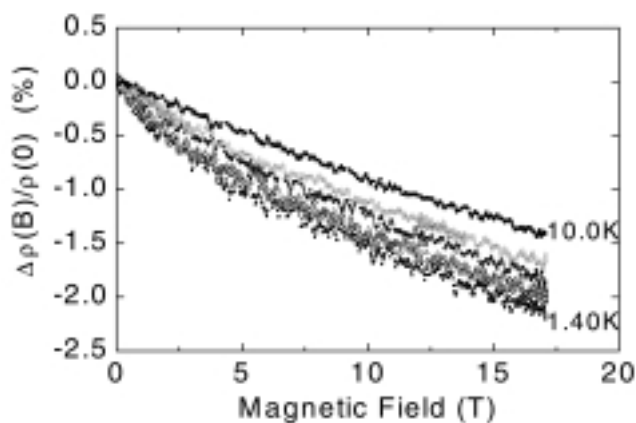


**Figure 2.** Transverse MR of sample H showing the lowest  $\rho(1.2\text{K})/\rho(300\text{K})$  value ( $T=1.40\text{ K}, 2.20\text{ K}, 4.00\text{ K}, 6.00\text{ K}$  and  $10.0\text{ K}$ ).

MR shows the square root dependence on  $B$  at  $T=1.50\text{ K}$ , and it becomes linearly dependent on  $B$  as  $T$  increases. At  $T=10\text{ K}$  (high  $T$ ), it becomes  $B^2$  dependent. (4) Transverse MR also exhibits the square root dependence on  $B$  at  $T=1.50\text{ K}$ , but it changes to be linearly dependent on  $B$  as  $T$  increases up to  $T=10\text{ K}$ . Further MR studies on a given piece of sample using the rotator are on going to clarify the orientation dependence of the MR.

<sup>1</sup> Park, Y.W., *et al.*, *Synth. Met.*, **96**, 81 (1998).

## Anomalous Spin Splitting Effects in $\alpha\text{-(ET)}_2\text{MHg(SCN)}_4$

Qualls, J.S., NHMFL/FSU, Physics

Brooks, J.S., NHMFL/FSU, Physics

Harrison, N., NHMFL

At low temperatures the organic compounds  $\alpha\text{-(ET)}_2\text{MHg(SCN)}_4$ , where  $M = \text{K, Rb, or Tl}$ , undergo a phase transition from a metallic (normal) state to a new electronic ground state. A density wave manifests and the Fermi surface reconstructs. The Fermi surface in the normal state is characterized by both one and two-dimensional components. After reconstruction, the one-dimensional components are removed and only the two-dimensional components remain (the exact details of the new configuration is debatable).

With the application of a magnetic field, Zeeman splitting occurs and two distinct sets of Landau levels form with a difference of energy equal to  $g\mu_B B$ . In this case,  $\mu_B$  is the Bohr magneton,  $g$  is the spin  $g$ -factor, and  $B$  is the magnitude of field. Since the two sets pass the Fermi surface at slightly different field strengths, an angular dependent damping factor is introduced. By measuring the angular dependence of the

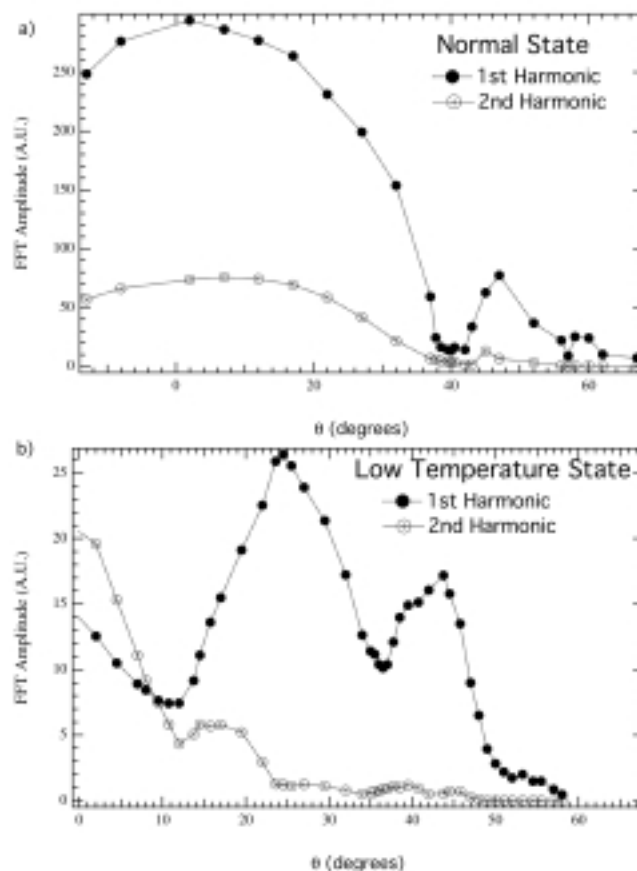


**Figure 1.** Harmonic content of the SdH oscillations as a function of  $\theta$  (a) Typical spin splitting effects are observed in the normal state. (b) Non L-K spin splitting is observed in the low temperature state.

harmonic content of the magnetic quantum oscillations in the magnetoresistance, also known as the Shubnikov-de Haas effect (SdH), the ratio  $m^*g$  can be extrapolated.<sup>1</sup> In particular we wish to obtain the effective mass parameter in both the normal and the low temperature state.

Measurements of the quantum oscillations in the  $M = \text{Rb}$  compound were performed in different field configurations up to 50 T at the NHMFL pulsed magnet facility at LANL. The angle  $\theta$  is defined as the angle away from the  $b^*$  axis, where  $b^*$  is defined to be normal to the most conducting plane. Figure 1 shows the angular dependence of the first and second harmonic content in both the normal and the low temperature ground state (as obtained from a FFT analysis of SdH spectrum). In Figure 1(a) the behavior of both harmonics can be modeled remarkably well by the semi-classical Lifshitz-Kosevich (LK) formula<sup>1</sup> describing Zeeman spin splitting. From the minimum positions along the angle  $\theta$ , this leads to the  $m^*g$  value of 3.83 (for the typical case  $g = 2$  and  $m^* = 1.9$ ).

Figure 1(b) shows the angular dependence of the harmonic content of the SdH spectrum in the low temperature state. Unlike in the normal state, the angular dependence of the harmonic content can not be described by the semi-classical LK formula for spin splitting. This is in contrast to claims made by others.<sup>2</sup> Not only is the angular dependence of the harmonic content anomalous but so is the field dependence of the harmonic content.<sup>3,4</sup> This effect only appears in transport measurements, as opposed to thermodynamic measurements like magnetization. This indicates a new type of transport mechanism arising as a result of the low temperature density wave that produces anomalous harmonic content.

<sup>1</sup> For review see Shoenberg, D., *Magnetic Oscillations in Metals* (Cambridge University Press, Cambridge, 1984).

<sup>2</sup> Sasaki, T. et al., *Phys. Rev. B*, 59, (1999).

<sup>3</sup> Kartsovnik, M.V. et al., *J. Physique*, 3, 1187 (1993).

<sup>4</sup> Uji, S., et al., *Phys. Rev. B*, 54, 9332 (1996).

## Competition Between Pauli and Orbital Effects in a Charge-Density Wave System

Qualls, J., NHMFL/FSU, Physics

Balicas, L., NHMFL and Venezuelin Institute for Scientific Research

Brooks, J.S., NHMFL/FSU, Physics

Harrison, N., NHMFL/LANL

Montgomery, L.K., Indiana Univ., Chemistry

Tokumoto, M., Electrotechnical Laboratory, Tsukuba, Japan

The Zeeman term  $g\mu_B B$  is believed to have a profound effect in a charge-density wave (CDW) system, usually described as the superposition of two sub-bands of opposite spins, because it only couples bands with same spin. In a magnetic field, the nesting wave vector (a Fermi Surface geometrical property of low dimensional electronic system) for each sub-band is different,

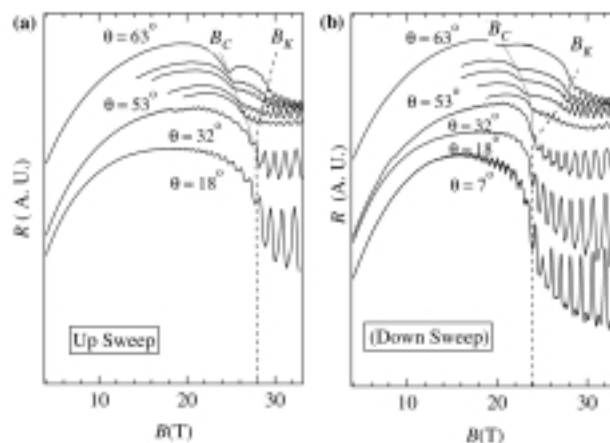


**Figure 1.** (a) Magnetoresistance of  $\alpha\text{-(ET)}_2\text{TiHg(SCN)}_4$  as a function of magnetic field  $B$ , for increasing field sweeps, at  $T = 40$  mK for several angles  $\theta$  between  $b^*$  and  $B$ . (b) For decreasing field sweeps. Curves are vertically displaced for clarity, the dotted lines indicating  $B_C$  and  $B_K$  are guides to the eyes.

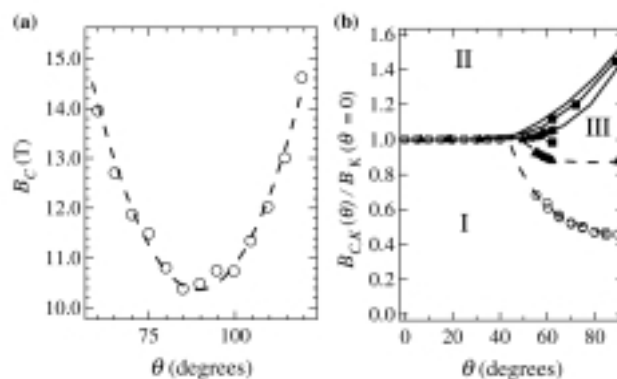


**Figure 2.** (a) Angular dependence of  $B_C$ . Dashed line is a fit to expression (1). (b) Resulting phase diagram:  $B_C$  and  $B_K$  as a function of  $\theta$ , for the TI (opened triangles) and K compounds (opened circles) at 40 mK, and the Rb compound (dots) at 500 mK.

consequently it is not possible to have the same nesting wave vector  $Q$  for both up-spin and down-spin bands.<sup>1</sup> The result is the suppression of a CDW state by the application of high magnetic fields: This effect is the analogue to the Pauli effect in superconductors. On the other hand, it is well established that the orbital motion of electrons in a magnetic field improves the nesting property of a density wave and is expected to increase its transition temperature.<sup>2</sup> The competition of both effects has been suggested to create a rich phase diagram under field.<sup>1</sup>

Here we present a detailed magnetotransport study in  $\alpha\text{-(ET)}_2\text{MHg(SCN)}_4$  (for  $M = \text{K, TI and Rb}$ ) compounds at high magnetic fields and low temperatures. In Figure 1 we show the magnetoresistance of  $\alpha\text{-(ET)}_2\text{TiHg(SCN)}_4$  as a function of  $B$  for increasing field sweeps (Figure 1(a)) as well as for decreasing field sweeps (Figure 1(b)) at  $T = 40$  mK for several angles  $\theta$  between  $B$  and  $b^*$ . The angular dependence of the magnetoresistance reveals two main features: The so-called kink field  $B_K$  moves toward higher values as  $\theta$  is increased and a new dip at a certain field  $B_C$ , whose position in field is angular dependent, appears above 45 degrees. Dotted and

dashed lines are guides to eyes. A similar behavior is observed in the K compound. In Figure 2(a)  $B_C$  as a function of  $\theta$  is displayed for  $\alpha\text{-(ET)}_2\text{KHg(SCN)}_4$  at  $T \sim 30$  mK. The dashed line is a plot to the following expression:

$$H_{cy} \sim H_c^0 \{1 + 0.088\eta^2\}^{1/2} \quad (1)$$

where  $\eta \equiv q_0/q_p = ebv_F \cos\theta / \mu_B$  is the ratio between the orbital and Pauli wave numbers which according to Zanchi et al.<sup>1</sup> defines a phase transition from the zero field CDW state labeled in Reference 1 as  $\text{CDW}_0$ , toward a new CDW phase:  $\text{CDW}_y$ . If we identify  $B_K$  as the critical field between  $\text{CDW}_0$  and the so-called  $\text{CDW}_x$  state, which is a CDW-SDW hybrid, the agreement with the theoretical description given in Reference 1 is excellent.

In Figure 2 we plot position in field of both  $B_C$  and  $B_K$ , normalized respect to  $B_K$ , as a function of  $\theta$  for the K compound (circles) at 30 mK, the Tl compound (solid triangles) at 40 mK and the Rb compound at 500 mK (solid squares). In this  $B$ - $\theta$  phase diagram we identify three regions: region I with  $\text{CDW}_0$ , region II with  $\text{CDW}_x$  and region III with  $\text{CDW}_y$  state. Clearly, the boundary between regions I and III and II and III is sample dependent.

<sup>1</sup> Zanchi, D., *et al.*, Phys. Rev. B **53**, 1240 (1996); McKenzie, R.H., cond mat/9706235 (1997).

<sup>2</sup> Gor'kov, L.P. and Lebed, A.G., J. Phys. Lett. (Paris), **45**, L433 (1984).

## Electronic Structure of the Organic Conductor $\alpha\text{-(ET)}_2\text{MHg(SCN)}_4$

Qualls, J.S., NHMFL/FSU, Physics

Brooks, J.S., NHMFL/FSU, Physics

Harrison, N., NHMFL

Balicas L., NHMFL and Venezuelan Institute for Scientific Research

Montgomery, L.K., Indiana Univ., Chemistry

Tokumoto, M., ETL, Japan

The organic compounds of  $\alpha\text{-(ET)}_2\text{MHg(SCN)}_4$ , where  $M = \text{K, Rb, or Tl}$ , have been intensively investigated over the past decade. Most of this is due to an anomalous electronic state that develops at low temperatures. This anomalous electronic state appears to be the onset of density wave formation, however to date there is no conclusive evidence identifying the type of density wave (DW). X-ray studies do not reveal a charge density wave (CDW) and NMR does not reveal a spin density wave (SDW). Not only is the nature of the density wave in question but the electronic structure and phase boundaries of the low temperature state are as well.<sup>1</sup> In attempts to map the phase boundaries and to gain insights into the low temperature state, a systematic study of the magnetoresistance has been performed. Measurements include the effect of field strength, field orientation, and temperature on the subject compound in all

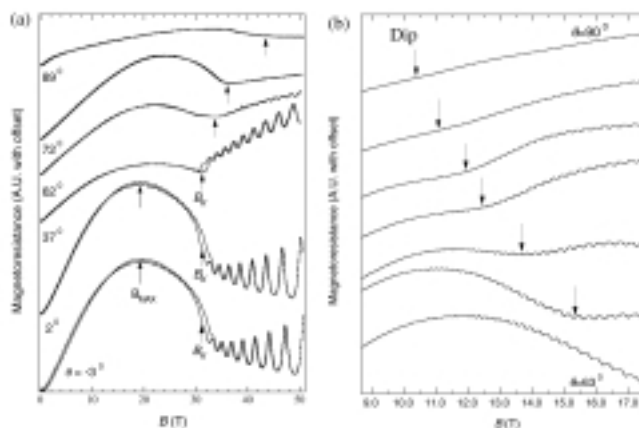


**Figure 1.** Typical measurements of the magnetoresistance as a function of field strength and orientation (a) Data on the  $M = \text{Rb}$  compound at 3 K reveals that  $B_K$ , the kink field, moves with angle  $\theta$ . (b) Data on the  $M = \text{K}$  compound at 0.05 K reveals the onset of a new orbital induced sub-phase. This sub-phase is responsible for the  $\theta$  dependence of  $B_K$  observed in Figure 1 (a).

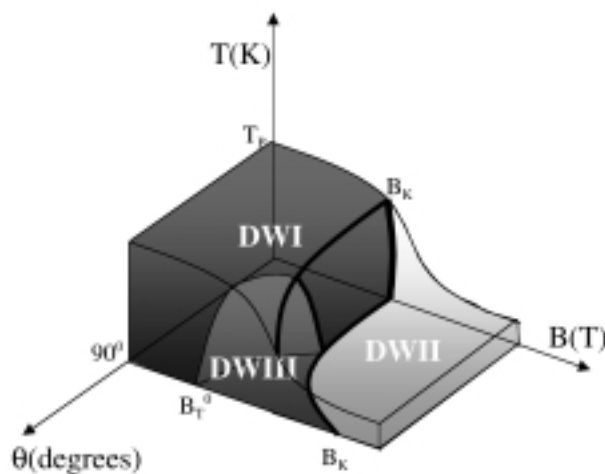


**Figure 2.** New electronic phase diagram based on temperature, field strength, and field orientation. Thin lines indicate a second order transition and thick lines indicate a first order transition.

electronic phases. Magnetic fields were generated at NHMFL using the 50 and 60 T pulse magnets at the Los Alamos facility and the 33 T resistive and 20 T superconducting magnets at the Tallahassee facility.

The normal state of the subject compounds is metallic and has a Fermi surface characterized by both quasi-one dimensional sheets and quasi-two dimensional cylinders.<sup>2</sup> At the temperature  $T_P$ , a low temperature electronic phase forms (DWI). ( $T_P = 8$  K, 10 K, and 12 K for  $M = \text{K, Tl, and Rb}$ , respectively). This results in a Fermi surface reconstruction. The Fermi surface of DWI is characterized by the original Fermi cylinders plus new pockets of closed Fermi surfaces. The angular dependent magnetoresistance oscillations (AMRO) exhibit a behavior characteristic of quasi-one dimensional Fermi sheets. The origin of the pockets or the precise orientation of the cylinders, which

generate the AMRO, is still debatable. As the field is increased, DWI is destroyed. Figure 1(a) shows typical data for the  $M = \text{Rb}$  salt at 3 K as a function of field and the angle  $\theta$ , where  $\theta$  is defined as the angle away from the least conductive axis. ( $\theta = 0^\circ$  corresponds to  $b^*$  axis and is normal to the most conductive planes). At the position marked  $B_{\text{max}}$ , the magnetoresistance begins to decrease and DWI begins to be quickly destroyed. Finally, at the field  $B_K$ , marked by a strong hysteretic kink in magnetoresistance, DWI evolves into a new electronic phase (DWII). DWII is more stable to the field strength and is not destroyed by highest measured fields at low temperatures. DWII has a Fermi surface almost identical to the normal state plus a new unexplained channel of highly metallic conductivity.

As seen in Figure 1(a),  $B_K$  moves as a function of  $\theta$ , for  $\theta > 60^\circ$ . This is the first reported case of  $B_K$  moving with field orientation and indicates the onset a new orbital induced sub-phase (DWIII). A dip in the magnetoresistance marks the phase boundary between DWI and DWIII. Figure 1(b) shows the dip as it appears in the  $M = \text{K}$  compound at 0.05 K at different  $\theta$  orientations. The dip moves to lower fields as the field approaches the in-plane position ( $\theta = 90^\circ$ ). In-plane anisotropy reveal that the Fermi surface in DWIII is similar to the normal state, however the angular dependent oscillations in the magnetoresistance (AMRO) is very similar to DWI.

Both the effective mass and Dingle temperature, as extrapolated from the behavior of the quantum oscillatory effects via the semiclassical Lifshitz-Kosevich formula, is different in every electronic phase. This supports a picture in which the electronic structure of the subject compounds can be clearly separated into four electronic phases (normal, DWI, DWII, DWIII). By compiling all of the data from pulsed and steady fields, the phase boundaries for the electronic states can be summarized as in Figure 2. Zanchi et al., predict that it is possible for a CDW to exist with complex sub-phases due to the interplay of orbital and Pauli effects.<sup>3</sup> Almost all aspects of the phase diagram in Figure 2 can be explained remarkably well in this CDW framework. This provides strong evidence for a CDW in the low temperature state. This work provides direct evidence of multiple electronic phases, extends the phase boundaries of the low temperature ground state, provides insights into the electronic structure for each phase, and indicates the feasibility of a CDW framework.<sup>4,5</sup>

<sup>1</sup> Brooks, J.S., *et al.*, in *Physical Phenomena at High Magnetic Fields II*, edited by Z. Fisk *et al.*, (world Scientific, Singapore, 1996).

<sup>2</sup> For a review of these compounds see Wosnitza, J., *Fermi Surfaces of Low Dimensional Organic Metals and Superconductors* (Springer-Verlag, Berlin, 1996).

<sup>3</sup> Zanchi, D., *et al.*, *Phys. Rev. B* **53**, 1240 (1996). Also, see a similar phase diagram by McKenzie, R. H., cond-mat/9706235.

<sup>4</sup> Qualls, J.S., Thesis, Florida State University, 1999.

<sup>5</sup> Qualls, J.S., *et al.*, submitted to *Phys. Rev. Lett.* 1999.

## Magnetoresistance of S-Type Helical Polyacetylene Doped with Iodine

Suh, D.-S., Seoul National Univ., Korea, Physics

Kim, T.J., Seoul National Univ., Korea, Physics

Park, Y.W., Seoul National Univ., Korea, Physics/NHMFL

Akagi, K., Univ. of Tsukuba, Inst. of Material Science, Japan

Shirakawa, H., Univ. of Tsukuba, Inst. of Material Science, Japan

Brooks, J.S., NHMFL/FSU, Physics

The two types of helical polyacetylene, R- and S-polyacetylene, differ in not only the helicity but also the degree of tightness of the twisted fiber structure.<sup>1</sup> Fibers in S-polyacetylene are more loosely twisted than in R-polyacetylene. Therefore the comparison between the transport properties of R- and S-polyacetylene is expected to give much information on the effect of the interfibrillar interaction in this polymeric system.

Figure 1a shows the lowest  $\rho_r (= \rho(1.2\text{K})/\rho(300\text{K}))$  data of S- and R-polyacetylene doped with iodine. The  $\rho_r$  value of R-polyacetylene is much lower than that of S-polyacetylene. In the repeated experiments, we cannot achieve the  $\rho_r$  value lower than 8.3 in the S-polyacetylene film. Figure 1b shows the magneto-resistance (MR) of S-polyacetylene. It forms a large

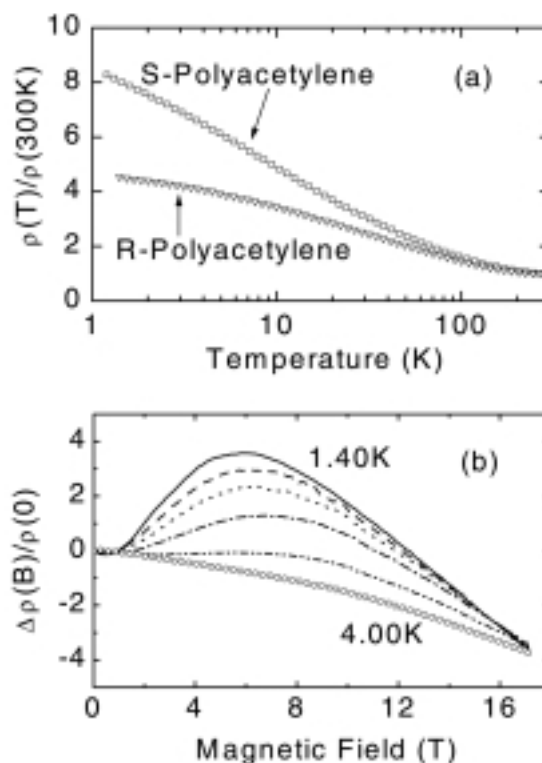


**Figure 1.** (a) Temperature dependence of resistivity normalized by the room temperature value of R- and S-polyacetylene. (b) Transverse MR of S-polyacetylene at  $T=1.40$  K, 1.60 K, 1.80 K, 2.20 K, 3.00 K and 4.00 K.



positive MR with a peak around 6 T and then goes to negative in the higher field region. When we compare this result to that of R-polyacetylene showing roughly the same  $\rho_r$  value, we can easily notice that the positive component in MR of S-polyacetylene is much larger than that of R-polyacetylene. The origin of this difference can be understood from the structural distinction between the R- and the S-polyacetylene film as following.

Without the magnetic field, the charge conduction happens mainly along the fiber. Under the magnetic field, however, the charge carriers can be deflected due to the field. Consequently, the interfibrillar interaction can enhance the charge delocalization under the magnetic field, which could be one of the origins of negative MR of highly conducting polyacetylene. If the coupling is weak, the charge delocalization cannot occur significantly and the charge carriers are confined within the given fiber. Therefore even though the zero field resistivity ratio is comparable, the larger positive MR could occur in S-polyacetylene from the effect of the weak interfibrillar interaction arising from the loosely twisted fibers.

**Acknowledgements:** This work was supported by KISTEP with 98-I-01-04-A-026, MOST, KOREA and by NSF-DMR-95-27035, and by the State of Florida.

<sup>1</sup> Akagi, K., *et al.*, Science, **282**, 1683 (1998).

## Magnetotransport Properties of R-Type Helical Polyacetylene Doped with Iodine

Suh, D.-S., Seoul National Univ., Korea, Physics

Kim, T.J., Seoul National Univ., Korea, Physics

Park, Y.W., Seoul National Univ., Korea, Physics/NHMFL

Akagi, K., Univ. of Tsukuba, Inst. of Material Science, Japan

Shirakawa, H., Univ. of Tsukuba, Inst. of Material Science, Japan

Brooks, J.S., NHMFL/FSU, Physics

We have investigated the electrical resistivity and the magnetoresistance (MR) of R-type helical polyacetylene<sup>1</sup> doped with iodine. The helical polyacetylene has two special features distinguishable from the traditional high-density film. One is that the size of fiber is approximately ~100 nm diameter that is much larger than that of the traditional one. The other is that the large fibers are twisted to form the ropes. R-polyacetylene has the counterclockwise helicity.

The zero-field resistivity ratio,  $\rho_r = \rho(1.2\text{K})/\rho(300\text{K})$ , of each sample is 4~14 as shown in Figure 1a, comparable to that of the stretched high-density film. It could be originated from the well-defined fiber structure. Figure 1b 1c and 1d show the MR of each sample. The MR in low field region changes systematically from negative to positive as the  $\rho_r$  value increases. The negative MR in the high field region looks similar, however, and its value at 17 T is almost the same for all three samples.

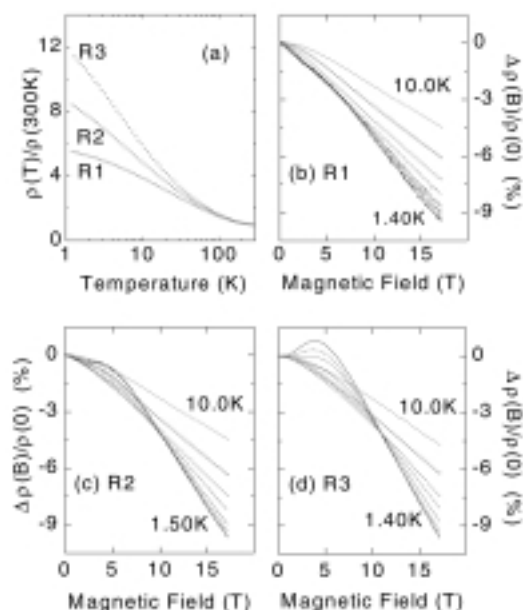


**Figure 1.** (a) Temperature dependence of resistivity normalized by the room temperature value. (b) (c) and (d) Transverse MR of each sample. Temperature is fixed at 1.40 K (1.50 K in (c)), 1.60 K, 1.80 K, 2.20 K, 2.50 K, 3.00 K, 4.00 K, 6.00 K, 10.0 K for each data.

When we analyze the observed MR data carefully, we find that the  $[\sigma(B)/T^{3/4}]$  vs.  $(B/T)$  plot shows the scaling behavior shown in Figure 2. If we assume the conductivity is additive, we can think of the data in Figure 2 as a combination of the two parts; the positive component with linear dependence shown as the background of a dashed line and the negative component with constant value at high  $B/T$  region.

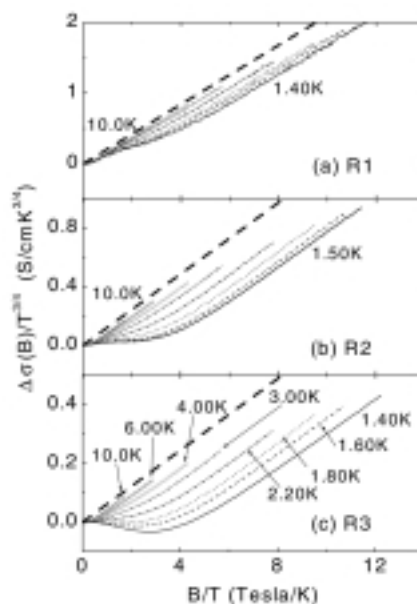


**Figure 2.** The  $\sigma(B)/T^{3/4}$  vs.  $(B/T)$  plots for iodine doped R-polyacetylene films. The thick dashed line shows the linear positive background indicating negative MR component.

Consequently, we can divide the MR into the positive one, sensitively dependent on the  $\rho_r$  in the low field region, and the negative one showing roughly linear B dependence in the high field region. The former can be interpreted as the spin-dependent variable-range-hopping model and the latter can be attributed to the localization effect in the disordered system. The behavior of the negative MR, however, is far from the conventional results predicted in the three-dimensional weak-localization theory. The inherent low dimensional characteristics of the polyacetylene system should be considered to explain these results.

Acknowledgements: This work was supported by KISTEP under the contract no. 98-I-01-04-A-026, MOST, KOREA, and by NSF-DMR-95-27035 and the State of Florida.

<sup>1</sup> Akagi, K., *et al.*, Science, **282**, 1683 (1998).

## Angle Dependence of the Upper Critical Field and Evidence for the Fulde-Ferrell-Larkin-Ovchinnikov State in the Organic Superconductor $\kappa$ -(BEDTTTF)<sub>2</sub>Cu(SCN)<sub>2</sub>

Symington, J.A., Univ. of Oxford, Physics

Nam, M.-S., Univ. of Oxford, Physics

Singleton, J., Univ. of Oxford, Physics

Ardavan, A., Univ. of Oxford, Physics

Blundell, S.J., Univ. Of Oxford, Physics

Harrison, N., LANL

Mielke, C.H., LANL

Kurmoo, M., Institut de Physique et Chimie des Matériaux de Strasbourg, (IPCMS), France

Day, P., The Royal Institution, London, U.K.

We have performed a detailed study of the dependence of the resistive upper critical field on the direction of the magnetic field B in the organic superconductor  $\kappa$ -(BEDT-TTF)<sub>2</sub>Cu(NCS)<sub>2</sub>.

<sup>1</sup> The measurements used a special two-axis rotation insert built in Oxford, which allows the sample to be orientated at any angle to B in-situ and at cryogenic temperatures; fields were provided by magnets at Tallahassee, LANL and Oxford. The orientation of the sample is defined by the polar angle  $\theta$  between B and the normal to the sample's bc planes and the azimuthal angle  $\phi$ ;  $\phi=0$  represents a plane of rotation of B containing b and the normal to the bc plane. Figure 1 (upper part) shows the  $\phi$  dependence of the in-plane ( $\theta=90^\circ$ ) resistive upper critical field defined by a zero magnetoresistance extrapolation ( $B_{MR \rightarrow 0}$ ) at temperatures of 4.2 K and 1.45 K. There is little or no  $\phi$  dependence of the critical field in spite of evidence of gap nodes characteristic of d-wave superconductivity.<sup>2,3</sup> Figure 1 (lower part) shows the full  $\theta$  and  $\phi$  dependence of  $B_{MR \rightarrow 0}$  at 1.45 K. The  $\theta$  dependence of

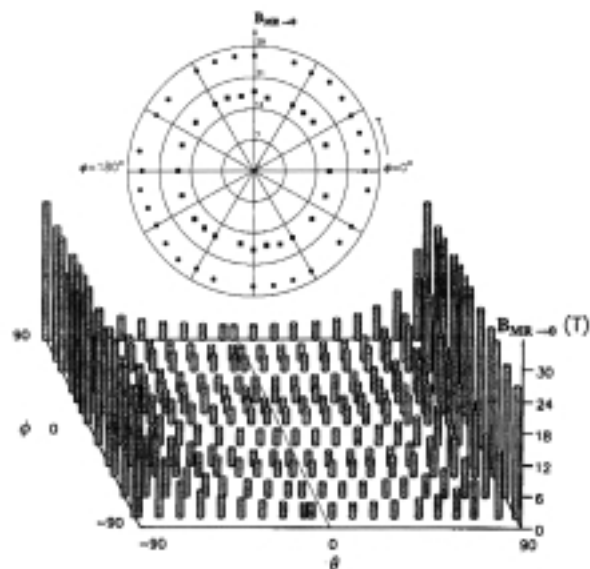


**Figure 1.** Upper part: azimuthal angle dependence of in-plane  $B_{MR \rightarrow 0}$  at  $T= 4.2$  K (filled squares) and 1.45 K (filled circles) in  $\kappa$ -(BEDT-TTF)<sub>2</sub>Cu(NCS)<sub>2</sub>. Lower part: the full angle dependence of  $B_{MR \rightarrow 0}$  at 1.45 K.

the measured critical fields can be described by Eqn. 1, which represents an anisotropic orbital limiting mechanism, combined with an isotropic Pauli paramagnetic limit.<sup>1</sup>

$$B_{c2}(\theta) = \frac{B_0}{\sqrt{\cos^2(\theta) + \alpha^2}} \quad (1)$$

Here  $B_0 = (1 + \alpha^2)B_{c2}(\theta=0)$ ,  $\alpha = B_0/B_{\text{spin}}$ , and  $B_{\text{spin}}$  is the limiting field due to the spin.<sup>1</sup> Eqn. 1 gives a good fit of the  $\theta$  dependence of  $B_{MR \rightarrow 0}$  for angles  $|\theta| < 86^\circ$ . However, the data for  $|\theta|$  closer to  $90^\circ$  do not follow the same dependence, and  $B_{MR \rightarrow 0}$  exceeds

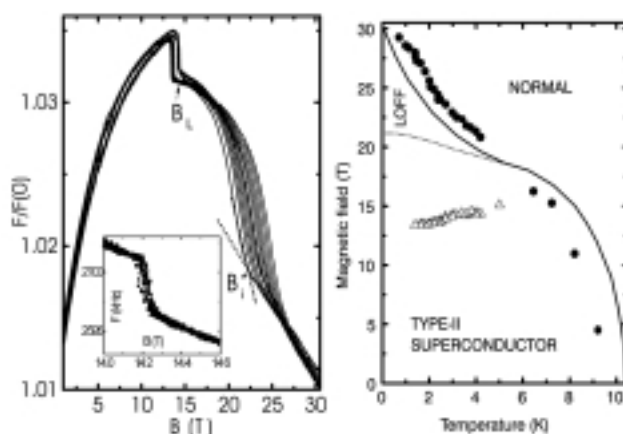


**Figure 2.** Left side: the normalized TCDS frequency vs. magnetic field for several temperatures  $T$  between 1.39 K and 4.2 K for the field parallel to the highly conducting layers. A sharp drop in frequency is seen at  $B_L \sim 14$  T, moving to lower fields as  $T$  decreases. The inflection at higher fields are associated with the upper critical field. The inset shows an enlargement at the region around  $B_L$ . Right side; temperature dependence of the fields  $B_1$  (triangles) and  $B_m$  (circles) compared with the theoretical FFLO phase diagram of Reference 3.

both the fitted  $B_{\text{spin}}$  and the Pauli paramagnetic limit<sup>1</sup> at 1.45 K and at 4.2 K.

It has been suggested<sup>4</sup> that such behavior could indicate the existence of a Fulde-Ferrell-Larkin-Ovchinnikov state, a state in which there is an attractive interaction between carriers with opposite spins on opposite sides of the Fermi surface, which leads to the formation of pairs with non zero total momentum;<sup>5,6</sup> further experiments were therefore carried out to check this proposal.<sup>7</sup> Single crystals were mounted within the coil of a tuned circuit differential susceptometer (TCDS)<sup>7</sup>. In the TCDS, the coil is part of a tuned circuit operating at  $\sim 3$  MHz. Changes in the magnetization and the differential susceptibility of the sample are detected as shifts in the frequency. The sample magnetoresistance was measured simultaneously. Samples were aligned with the field parallel to the highly conducting planes to within  $0.1^\circ$ .<sup>4</sup> The TCDS frequency is shown in Figure 2 (left side) for temperatures in the range 1.39 K to 4.2 K. The upper critical field was observed for each temperature as a point of inflection,  $B_i$ . The values of  $B_i$  agree well with simultaneous measurements of the resistive midpoint fields  $B_m$ .<sup>1</sup> However, the most striking feature of the data was a sharp drop,  $B_L$ , which remains at  $\sim 14$  T for all temperatures. The sharpness of this feature suggests that it is a first-order transition.<sup>7</sup>

Figure 2 (right side) shows the temperature dependence of  $B_m$  and  $B_i$  plotted alongside a theoretical phase diagram for the FFLO state.<sup>4</sup> The data in the figure bear a strong qualitative resemblance to the theoretical phase diagram, as the drop at  $B_L$  is indicative of the first order phase transition (c.f. the theoretical first-order phase transition between the superconducting and FFLO states). Moving away from the in-plane geometry allows the number of closed quasiparticle orbits to increase and so orbital mechanisms destroy the superconductivity. The drop in the response of the TCDS is only clearly visible when the field is within  $4^\circ$  of parallel to the conducting layers.

<sup>1</sup> Nam, M.-S., *et al.*, J. Phys.:Condens. Matter, **11**, L477 (1999).

<sup>2</sup> Schmalian, J., Phys. Rev. Lett., **81**, 4232 (1998).

<sup>3</sup> Schrama, J.M., *et al.*, Phys. Rev. Lett., **83**, 3041 (1999).

<sup>4</sup> Shimahara, H., Phys. Rev. B, **50**, 12760, (1994).

<sup>5</sup> Fulde, P. and Ferrell, R.A., Phys. Rev., **135**, A550, (1964).

<sup>6</sup> Larkin, I. and Ovchinnikov, Y.N., Zh. Eksp. Teor. Fiz., **47**, 1136, (1964).

<sup>7</sup> Symington, J.A., *et al.*, Phys. Rev. Lett. submitted; APS preprint /eprint/gateway/eplist/aps1999aug23\_001.

## Conductivity Studies on the Organic Superconductor $\beta''$ -( $\text{ET}$ ) $_2\text{SF}_5\text{CH}_2\text{CF}_2\text{SO}_3$

Symington, J.A., Univ. of Oxford, Physics  
 Edwards, R.S., Univ. of Oxford, Physics  
 Rzepniewski, E., Univ. of Oxford, Physics  
 Singleton, J., Univ. of Oxford, Physics  
 Ardavan, A., Univ. of Oxford, Physics  
 Schleuter, J., Argonne National Laboratory

We report cyclotron resonance (CR) and magnetoresistance measurements on  $\beta''$ -( $\text{ET}$ ) $_2\text{SF}_5\text{CH}_2\text{CF}_2\text{SO}_3$ .<sup>1</sup> This is the first

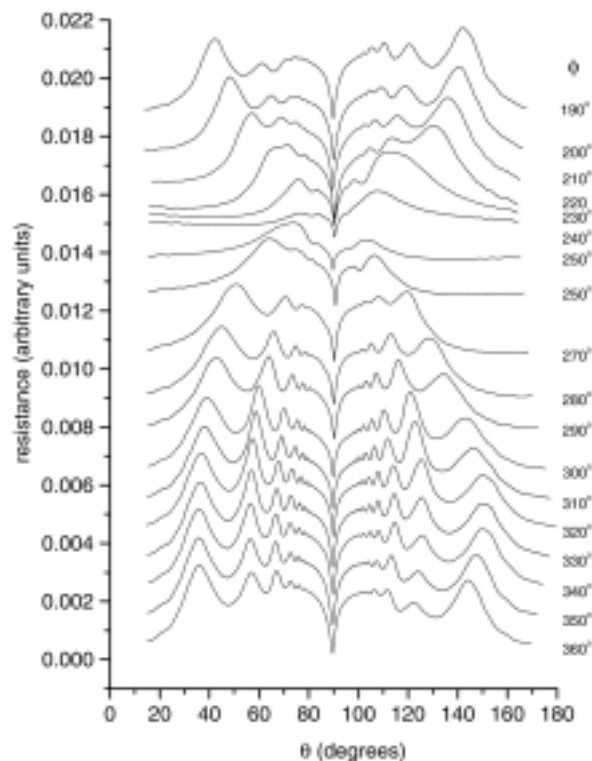


**Figure 1.** Angle dependent magnetoresistance oscillations at 10T for  $\beta''$ -( $\text{ET}$ ) $_2\text{SF}_5\text{CH}_2\text{CF}_2\text{SO}_3$  ( $T=1.3$  K).

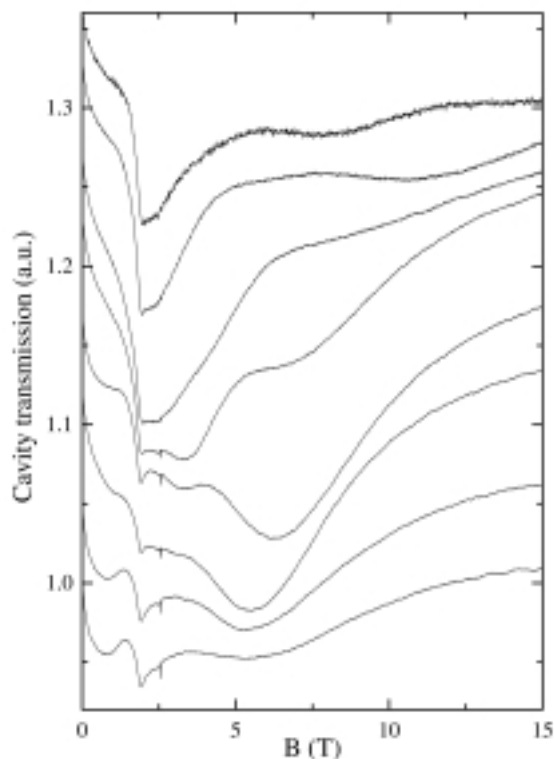
entirely organic superconductor to be synthesized. Extended Hückel calculations<sup>2</sup> predict a Fermi surface (FS) consisting of a pair of quasi-one-dimensional sheets and a quasi two-dimensional (Q2D) pocket.

Figure 1 shows the  $\theta$  dependence ( $\theta$  is the angle between the normal to the Q2D planes and the magnetic field) of the resistance for a field of 10 T and several values of  $\phi$  ( $\phi$  defines the plane of rotation of the field). The data show clear angle-dependent magnetoresistance oscillations (AMROs) with sharp maxima, suggesting that they are caused by a Q2D FS section. A newly developed technique<sup>3</sup> suggests that this pocket has a cross-section shaped like a highly elongated diamond.

High frequency conductivity studies were also carried out. The sample was placed inside a rectangular cavity (71.2 GHz) that can rotate with respect to the applied field (i.e. change the angle  $\theta$ ). A measurement of the bulk conductivity is possible due to the large skin depth when the H-field of the GHz radiation is parallel to the Q2D planes. Figure 2 shows field sweeps for different  $\theta$ . The cavity background is seen at about 2 T. At intermediate fields, several broad resonances can be seen. Plotting the position of the main resonance versus  $\theta$ , it can be seen that it is symmetrical about  $\theta = 0$ , having the behavior expected of a CR. Other resonances, which appear at about half or a third of the field of the main CR, are harmonics. The main CR fits to an effective mass of  $m_{\text{CR}}^* = 2.26 \pm 0.03 m_e$ .

The observation of cyclotron harmonics has been predicted by Blundell *et al.*,<sup>4</sup> who suggested the presence of odd harmonics when the FS cross-section is very non-elliptical. The





**Figure 2.** GHz conductivity of  $\beta''$ -(ET) $_2$ SF $_5$ CH $_2$ CF $_2$ SO $_3$ ; field sweeps between 0 and 15 T, showing the transmission through the resonant cavity. Sweeps have been normalized at 0 T and offset for clarity. Angles from  $\theta = 70^\circ$  at the top to  $0^\circ$  at the bottom of the figure in ten degree steps are shown.

second harmonic suggests an effect similar to that predicted by Hill,<sup>5</sup> who attributed such frequencies to the corrugations of the Fermi cylinders in the interplane (low conductivity) direction. Comparing the mass determined from the temperature dependence of magnetic quantum oscillations,  $m^* = 2.0 \pm 0.1 m_e$ , to the mass measured in the CR experiment,  $m_{CR}^*$ , we see that  $m_{CR}^* > m^*$  for this material. Thus it appears that the predictions<sup>6</sup> of a large enhancement of  $m^*$  over  $m_{CR}^*$  do not hold. Recent Hubbard-model calculations appear to support these experimental observations.<sup>7</sup>

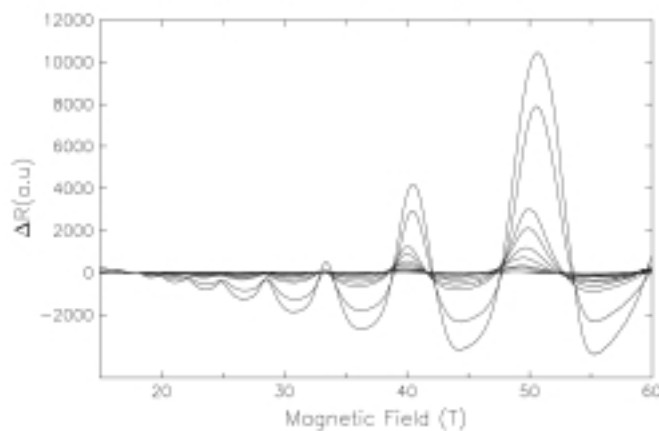


**Figure 3.** Temperature dependence of the oscillatory component of the interplane magnetoresistance of  $\beta''$ -(BEDT-TTF) $_2$ SF $_5$ CH $_2$ CF $_2$ SO $_3$ . (From the top,  $T = 0.59, 0.94, 1.48, 1.58, 1.91, 2.18, 2.68, 3.03, 3.38, 3.80$ , and  $4.22$  K).

Figure 3 shows the temperature dependence of the Shubnikov-de Haas (SdH) oscillations recorded in pulsed magnetic fields; the background classical magnetoresistance is subtracted in this figure. The SdH frequency is in good agreement with the AMRO data. In  $\alpha$ - or  $\kappa$ - phase salts of BEDT-TTF, the amplitude of the SdH oscillations usually saturates in a predictable manner with decreasing temperature. In  $\beta''$ -(BEDT-TTF) $_2$ SF $_5$ CH $_2$ CF $_2$ SO $_3$ , however, the amplitude of quantum oscillations continues to show a dramatic increase with decreasing temperature. This behavior may be related to charge localization between the highest Landau levels near the quantum limit; at 60 T, the highest occupied Landau level has the quantum number  $L=3$ . Another possibility is that the nesting of the quasi-one-dimensional (Q1D) Fermi-surface section is causing a field-induced transition similar to that in  $\beta''$ -(BEDT-TTF)AuBr $_2$ .<sup>8</sup> The AMRO experiments, however, do not detect signs of the Q1D Fermi surface or any change which might be expected if a field-induced transition occurred. A comprehensive model for the magnetoresistance is under development.

- <sup>1</sup> Edwards, R.S., to be published
- <sup>2</sup> Geiser, *et al.*, J. Am. Chem. Soc., **118**, 9996 (1996).
- <sup>3</sup> Blundell, *et al.*, to be published.
- <sup>4</sup> Blundell, *et al.*, Phys. Rev. B, **55**, R6129 (1997).
- <sup>5</sup> Hill, S., Phys. Rev. B., **55**, 4931 (1997).
- <sup>6</sup> Kohn, W., Phys. Rev., **123**, 1242 (1961).
- <sup>7</sup> Kanki, K. *et al.*, J. Phys. Soc. Jpn., **66**, 1103 (1997).
- <sup>8</sup> House, A.A., Phys. Rev. B, **53**, 9127 (1996).

## Fermiology of the Organic Superconductor $\beta''$ -(BEDT-TTF) $_2$ SF $_5$ CH $_2$ CF $_2$ SO $_3$

Wosnitza, J., Universität Karlsruhe, Germany,  
Physikalisches Institut

Harrison, N., NHMFL/LANL

Qualls, J.S., NHMFL/FSU, Physics

Brooks, J.S., NHMFL/FSU, Physics

Schlueter, J.A., Argonne National Laboratory

Kini, A.M., ANL

Geiser, U., ANL

Winter, R.W., Portland State Univ., Chemistry

Gard, G.L., Portland State Univ., Chemistry

The Fermi surface (FS) of the organic superconductor  $\beta''$ -(BEDT-TTF) $_2$ SF $_5$ CH $_2$ CF $_2$ SO $_3$  ( $T_c = 4.5$  K, BEDT-TTF = bisethylenedithio-tetrathiafulvalene) consists of a small quasi-two-dimensional (2D) hole pocket and a pair of wavy 1D bands.<sup>1</sup> The 2D FS has been observed experimentally both by Shubnikov-de Haas (SdH) and by de Haas-van Alphen (dHvA) measurements.<sup>1,2</sup> Thereby an oscillation frequency of about 200 T was found that corresponds to a FS area of about 5% of the first Brillouin zone. In high-field experiments in static fields a highly unusual temperature and field dependence of the SdH signal occurs.<sup>3</sup> Detailed dHvA experiments up to 28 T



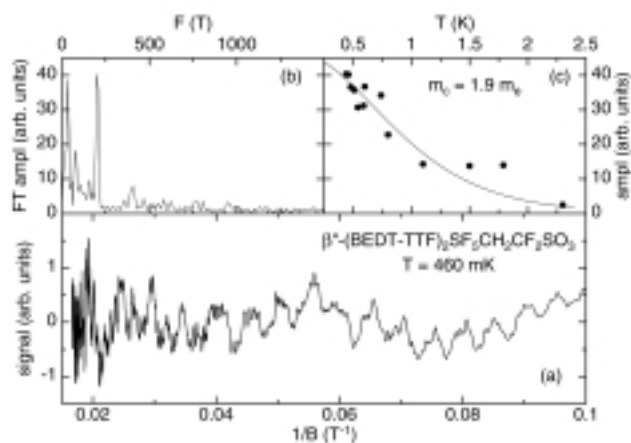


**Figure 1.** (a) Raw pick-up signal detected on the rising side of a 61 T pulse. (b) Fourier transformation of the signal with the fundamental dHvA frequency  $F_0 = 200$  T. (c) Temperature dependence of the fundamental dHvA amplitude.

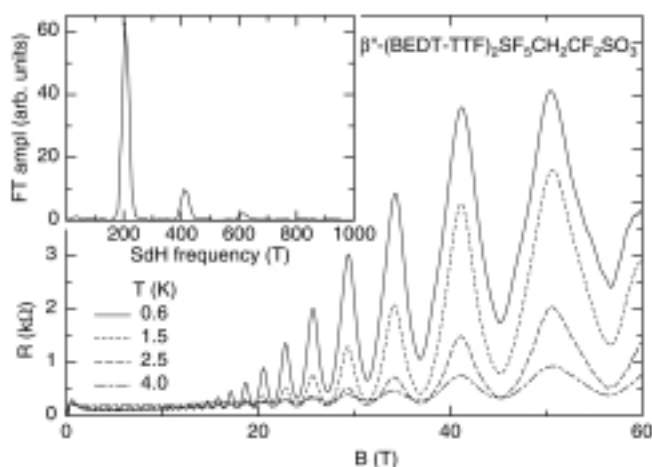


**Figure 2.** Field dependence of the resistivity up to 60 T at different temperatures with very strong SdH oscillations which saturate at the highest field and lowest temperatures. The inset shows the Fourier transformation of the data at  $T = 0.6$  K.

showed that the material behaves exactly like a 2D electron gas with fixed chemical potential.<sup>4</sup>

The present experiment was initiated to study these effects in more detail at even higher fields in order to drive the system close to the quantum limit (with only 3 Landau levels inside the FS at 60 T). Figure 1a shows the induced voltage on the rising side of a 61 T pulse as a function of the reciprocal field. The excellent sensitivity of the setup allowed to detect the very low dHvA frequency of about 200 T (see the Fourier transformation in Figure 1b) up to about 2.3 K. At higher fields the signal becomes more noisy due to the decreasing sweep rate  $B/\dot{t}$  close to the maximum field. From the temperature dependence of the dHvA amplitude an effective mass of  $m_c = 1.9 m_e$  is obtained (Figure 1c) in line with low-field experiments.<sup>1,2</sup>

For the transport data (Figure 2) we observe a strongly increasing background magnetoresistance which does not saturate even at the highest fields. Superimposed on this steady part, huge SdH oscillations are visible which do not behave as expected

from the dHvA data and from the theory for a 2D electron gas.<sup>4</sup> This shows clearly that an analysis of SdH data is not straightforward for the organic metals and that a refined theory is necessary to describe the observed signal at very high fields correctly.

As a final point we note that only one fundamental oscillation frequency occurs in the dHvA and SdH data with no indication of a magnetic breakthrough. This indicates that the calculated band structure,<sup>1</sup> which predicts a rather small gap between the closed 2D band and the open 1D bands, has to be modified.

- <sup>1</sup> Beckmann, D., *et al.*, Eur. Phys. J. B, **1**, 295 (1998).
- <sup>2</sup> Wosnitza, J., *et al.*, Physica B, **246-247**, 104 (1998).
- <sup>3</sup> Wosnitza, J., *et al.*, NHMFL 1998 Annual Report, p 168.
- <sup>4</sup> Wosnitza, J., *et al.*, to be published.

## Quasi-Two-Dimensional Spin-Split Fermi-Liquid Behavior of $\kappa$ -(BEDT-TTF)<sub>2</sub>I<sub>3</sub>

Wosnitza, J., Universität Karlsruhe, Germany,  
Physikalisches Institut

Harrison, N., NHMFL/LANL

Qualls, J.S., NHMFL/FSU, Physics

Brooks, J.S., NHMFL/FSU, Physics

Balthes, E., Universität Stuttgart, Physikalisches Institut

Schweitzer, D., Universität Stuttgart, Physikalisches Institut

The organic superconductor  $\kappa$ -(BEDT-TTF)<sub>2</sub>I<sub>3</sub> is characterized by an exceptionally pronounced two dimensionality (2D) of its electronic bandstructure. While the behavior of the magnetic quantum oscillations in this material conforms mostly to standard models at low magnetic fields,<sup>1</sup> strong deviations from these models, i.e., an apparent reduction of the effective mass, were observed in Shubnikov-de Haas (SdH) experiments at higher magnetic fields.<sup>2</sup>

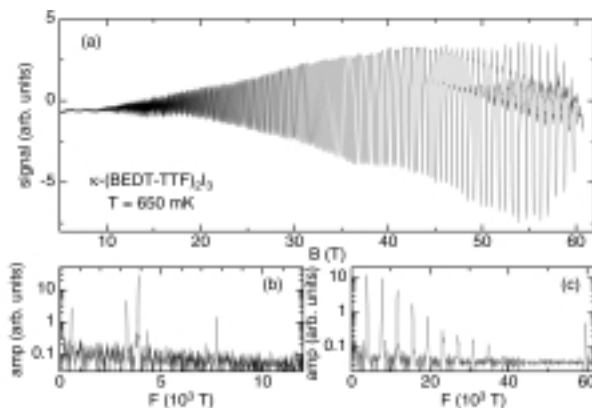


**Figure 1.** (a) Raw signal detected on the falling side of a magnetic field pulse. The Fourier transformations in  $1/B$  space for the field intervals  $10 < B < 40$  T (b) and  $40 < B < 61$  T (c).

We measured both the magnetization and the magnetoresistance in pulsed magnetic fields extending to 60 T and in static fields up to 20 T at very low temperatures down to 30 mK.<sup>3</sup> Figure 1a shows an example of an induced voltage signal. The Fourier transformation of the data below 40 T (Figure 1b) displays a dHvA frequency of 575 T corresponding to the so-called  $\alpha$

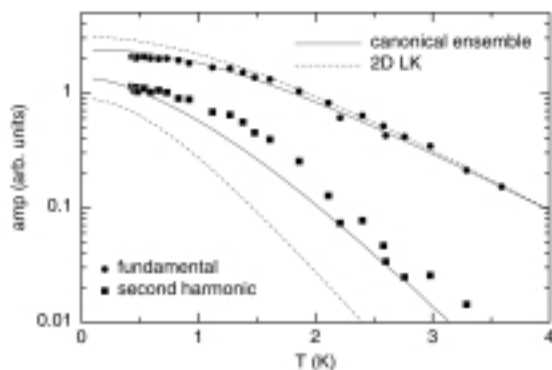


**Figure 2.** A comparison of the temperature dependences of the measured dHvA amplitudes with results using a numerical model (solid lines) and the LK theory.

pocket of the Fermi surface (FS) and the much larger frequency of 3875 T due to the breakdown  $\beta$  orbit. In many ways the oscillations below about 40 T reproduce the behavior seen in previous studies, with the exception of a  $\beta$ - $\alpha$  frequency which might be due to the oscillatory chemical potential in this 2D material. At higher magnetic fields the salt is taken deep into the magnetic-breakdown regime with a rich harmonic content of

the oscillations and finally a double-peak structure developing (Figure 1c). The latter structure is a result of well-resolved spin-split Landau levels in strong magnetic fields.

In contrast to the SdH effect, the oscillatory magnetization is a thermodynamic function of state, and is therefore able to probe the Fermi-liquid ground state directly. From the measured temperature dependences of the dHvA-oscillation amplitudes in pulsed field down to 0.4 K and in static fields down to 30 mK we obtain lower-than-expected effective masses when we fit the usual Lifshitz-Kosevich (LK) temperature reduction factor. At lower fields and higher temperatures the low-field value  $m_c = 3.9 m_e$ <sup>[1]</sup> is extracted. While the sign of the apparent mass change is in agreement with our and previous SdH studies,<sup>2</sup> this change is much more acute in the SdH signal. Deviations from the LK behavior due to a fixed chemical potential can be calculated quantitatively by use of a numerical model.<sup>4</sup> In the present case the effect of spin splitting is prominent and has to be taken into account properly. Figure 3 shows our experimental data for the fundamental and second harmonic of the dHvA amplitudes in comparison to the relative temperature dependences obtained from the numerical calculations by use of parameters extracted at low fields (solid lines) and with those of the LK theory (dashed lines). The numerical model describes the experimental dHvA data perfectly well.

<sup>1</sup> Heinecke, M., *et al.*, Z. Phys. B, **93**, 45 (1993).

<sup>2</sup> Balthes, E., *et al.*, Z. Phys. B, **99**, 163 (1996); Synth. Metals 94, 3 (1998).

<sup>3</sup> Harrison, N., *et al.*, Phys. Rev. B, **58**, 10248 (1998).

<sup>4</sup> Harrison, N., *et al.*, Phys. Rev. B, **54**, 9977 (1996).

## SEMICONDUCTORS

### Large Magnetoresistance of Silver Selenide in a Pulsed Field

Betts, J.B., NHMFL/LANL

Balakirev, F.F., NHMFL/LANL

Boebinger, G.S., NHMFL/LANL

Rosenbaum, T.F., Univ. of Chicago, Physics

Saboungi, M.-L., Argonne National Laboratory

Schynders, H., ANL

Silver chalcogenides exhibit promising characteristics for possible use as magnetoresistive devices because of their large magnetoresistance (MR).  $\text{Ag}_2\text{S}$ ,  $\text{Ag}_2\text{Se}$  and  $\text{Ag}_2\text{Te}$  are narrow-gap self-doped degenerate n-type semiconductors that show no appreciable MR. Previous investigations have shown that slight alterations in stoichiometry lead to a marked increase in magnetic response.<sup>1,2</sup> Increases in resistivity up to 200% at 5.5 T have been observed. The MR is found to be unusually linear from a few mT up to several T.<sup>1</sup>

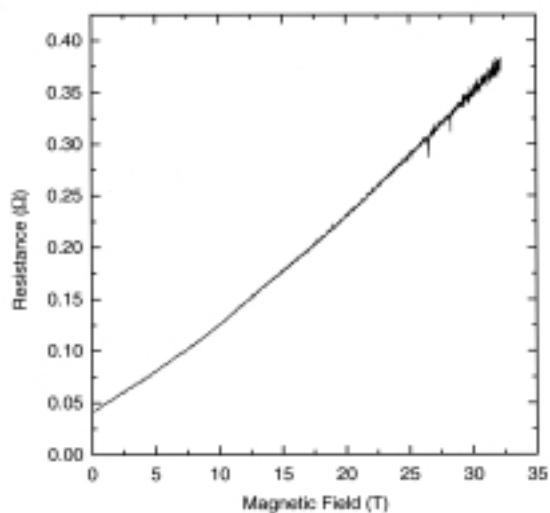


**Figure 1.** Magnetoresistance of  $\text{Ag}_{2-\delta}\text{Se}$  at 1.5 K.

We investigated the magnetoresistive response in the off-stoichiometric Se-rich compound  $\text{Ag}_{2-\delta}\text{Se}$  in pulsed magnetic fields up to 35 T. In this compound the electron density in the conduction band is largely determined by the stoichiometric